Metabolic and regulatory insights from the experimental Horizontal Gene Transfer of the aurofusarin and bikaverin gene clusters to Aspergillus nidulans

de Reus, Elise; Nielsen, Mikkel Rank; John Nordmand Frandsen, Rasmus

Published in:
Molecular Microbiology

DOI (link to publication from Publisher):
10.1111/mmi.14376

Publication date:
2019

Document Version
Accepted author manuscript, peer reviewed version

MISS ELISE DE REUS (Orcid ID : 0000-0001-6449-2014)

Article type : Research Article

Metabolic and regulatory insights from the experimental Horizontal Gene Transfer of the aurofusarin and bikaverin gene clusters to *Aspergillus nidulans*

Elise de Reus (1), Mikkel Rank Nielsen (2), Rasmus John Normand Frandsen (1) *

1) Department of Biotechnology and Bioengineering, Technical University of Denmark, Kgs. Lyngby, Denmark
2) Department of Chemistry and Bioscience, Aalborg University, Esbjerg, Denmark

*Corresponding author
rasf@bio.dtu.dk
+45 22541435

Key words:
Horizontal gene transfer
Secondary metabolism
Gene clusters
Gene Expression Regulation, Fungal
Ascomycota

Running title:
Experimental horizontal gene transfer in *A. nidulans*

Summary

We staged the transfer of the aurofusarin and bikaverin biosynthetic gene clusters (BGCs) to *Aspergillus nidulans* with the aim of gaining functional insights into dynamics immediately following a horizontal gene transfer (HGT) event. While the introduction of both BGCs resulted in the production of detectable pathway metabolites in *A. nidulans*, the transferred aurofusarin BGC formed dimeric shunt products instead of aurofusarin. This was linked to low transcription of the cluster activator and insufficient activity of tailoring enzymes, demonstrating how a shift of the pathway bottleneck after HGT can result in metabolic innovation. The transferred bikaverin BGC readily produced bikaverin, providing a model system for studying the conservation of regulatory responses to environmental cues. Conserved PacC-mediated pH regulation of the bikaverin BGC was observed between

original host *Fusarium fujikuroi* and *A. nidulans*. Contrary to strong nitrogen responses described in other hosts, the BGC appeared unresponsive to environmental nitrogen in *A. nidulans*. While *F. fujikuroi* and *A. nidulans* both form chlamydospore-like structures when exposed to ralsolamycin, specific induction of the bikaverin BGC was not observed in *A. nidulans.* We propose that the presence of compatible cis-regulatory elements in BGCs facilitates regulatory conservation after transfer, without which the chromosomal context would dictate expression.

Key words
Horizontal gene transfer
Secondary metabolism
Gene clusters
Gene Expression Regulation, Fungal
Ascomycota

Introduction

With the falling costs of whole genome sequencing, comparative genomics has emerged as a vibrant discipline that explores the genetic diversity across an increasing number of fungal species and genera (Brown and Proctor, 2016; de Vries *et al.*, 2016; Nielsen *et al.*, 2017; Kjærbølling *et al.*, 2018; Vesth *et al.*, 2018). A hallmark trait of fungal genomes is their large number of Biosynthetic Gene Clusters (BGCs); clusters of genes that encode the enzymes necessary for the production, modification, transport, and regulation of one or more specialized molecules, often secondary metabolites (SecMets). As newly sequenced genomes are mined for BGCs using various algorithms (Khaldi *et al.*, 2010; Vesth *et al.*, 2016; Weber *et al.*, 2017), an increasing number of BGCs is found to be distributed irregularly across genera and species (Khaldi *et al.*, 2008; Slot and Rokas, 2011; Campbell *et al.*, 2012; Campbell *et al.*, 2013; Proctor *et al.*, 2013; Sieber *et al.*, 2014; Bonham *et al.*, 2017). Consequently, Horizontal Gene Transfer (HGT) between- and into filamentous fungi is now recognized as an important source of genetic innovation (Rosewich and Kistler, 2000; Keeling, 2009; Richards *et al.*, 2011; Soanes and Richards, 2014; Husnik and McCutcheon, 2018), where the self-sustaining nature of BGCs is suggested to increase their chances of surviving HGT (Wisecaver *et al.*, 2014; Wisecaver and Rokas, 2015). One example of the far-reaching implications that HGT can have is the transfer of the ToxA virulence factor from the wheat pathogen *Pyrenophora tritici-repentis* to the pathogen *Stagonospora nodorum* in the 1940's that resulted in the outbreak of a new wheat disease (Friesen *et al.*, 2006).

Compared to the many studies that generate *in silico* insights into the evolutionary role of HGT, relatively few studies have experimentally demonstrated the implications of acquiring a new genetic trait. Alongside a handful of examinations of the barriers and facilitators of HGT in prokaryotes (Isobe *et al.*, 2004; Sorek *et al.*, 2007; Park and Zhang, 2012), there are a few compelling studies dealing with the situation in fungi and their secondary metabolism. One example is the study by Ma et. al, who demonstrated the relative ease with which horizontal transfer of mobile chromosomes can confer pathogenicity between asexual strains of *Fusarium* (Ma *et al.*, 2010). Another is the ancient transfer of the bikaverin cluster from *Fusarium* to *Botrytis* where complementation studies and metabolite analysis showed that several isolates of *B. cinerea* contain a functional bikaverin cluster (Schumacher *et al.*, 2013). Comparative analysis of the regulation before and after transfer showed that the regulatory proteins Bik4 and Bik5 remained active even after degradation of the rest of the cluster (Campbell *et al.*, 2013). Recently, Spraker et al. described involvement of the *bik* cluster in a conserved response to *Ralstonia solanacearum* by *F. fujikuroi* and *B. cinerea* (Spraker *et al.*, 2018). In this way, empirical insights are valuable in deepening our understanding of the forces that influence the success of HGT.

Ironically, experimental transfer of BGCs is frequently conducted for an altogether different purpose: the discovery of products from newly identified BGCs. The linking of BGC to metabolites can be a notoriously difficult endeavor, as species can be difficult to cultivate and many BGCs are silent under laboratory conditions (Brakhage and Schroeckh, 2011). While culturing under different conditions following the OSMAC approach (Bode *et al.*, 2002) is still used as a tool, efforts have recently shifted to high throughput heterologous expression strategies. In one variant, BGCs from various species were transferred to *A. nidulans* on Fungal Artificial Chromosomes (FACs) (Clevenger *et al.*, 2017). Another strategy is heterologous expression (HEX) in *S. cerevisiae* (Harvey *et al.*, 2018). While these methods have successfully identified numerous new metabolites, it is a public secret that many unsuccessful transfers, in the sense that they not result in the production of metabolites, are left unreported (Keller, 2019). Among the outstanding questions in the field of fungal secondary metabolism are: what is the effect of phylogenetic distance on the likelihood of BGC expression (Clevenger *et al.*, 2017)? And why do BGCs form products in some species but not others (Rokas *et al.*, 2018)?

Using an experimental approach to describe the immediate metabolic and regulatory effects of whole cluster transfer could help to address such questions. In the current study, we staged the inter-genus transfer of the aurofusarin and bikaverin gene clusters, two model BGCs from *Fusarium spp.,* to the model organism *A. nidulans*. Through investigation at the transcriptional, protein, and metabolite level we generated insights into how a BGC functions immediately following a HGT event. Our work highlights how HGT can shift the bottleneck of a SecMet pathway, which could diminish the evolutionary success of the event or provide an avenue for metabolic innovation in the recipient. Furthermore, it demonstrates examples of factors that dictate whether the BGCs' response to environmental cues are retained after HGT. We propose that compatible cis-regulatory elements aid the conservation of regulation of transferred genes, increasing the likelihood of the transferred cluster maintaining its function. Without such elements, the integration locus of the transferred DNA is proposed to be the main determinant for expression of the BGC.

Results

Selection and transfer of two model BGCs to *A. nidulans* as experimental HGT recipient

To experimentally gain insight into the immediate effects following a whole-BGC HGT event and the barriers for successful HGT of gene clusters, we reviewed literature to identify well-characterized BGCs that could be used as models in the study. We selected the aurofusarin gene cluster from *Fusarium graminearum* and the bikaverin gene cluster from *Fusarium fujikuroi* for the whole-BGC transfer. Aurofusarin and bikaverin are red mycelial pigments with polyketide-synthase derived napthopyrone backbones, whose biochemical pathways, cluster boundaries, and gene regulation have been thoroughly characterized (Linnemannstöns *et al.*, 2002; Frandsen *et al.*, 2006; Wiemann *et al.*, 2009; Frandsen *et al.*, 2011; Arndt *et al.*, 2015). A schematic overview of the BGCs and the functionalities the genes encoded can be found in Supplementary Figure 1. The bikaverin cluster was naturally transferred from *Fusarium* to *B. cinerea* and the cluster's response to biotic and abiotic cues has been described in both organisms (Campbell *et al.*, 2012; Schumacher *et al.*, 2013; Spraker *et al.*, 2018).

A key second component of the analysis was to choose a suitable acceptor organism for the entire BGC-transfer. For this we selected the model organism *Aspergillus nidulans* which is well-characterized with respect to morphology, physiology, genetics and metabolism and for which a versatile set of genetic engineering methods are available. More specifically, we

chose to use a pigment-deficient *Aspergillus nidulans* strain (Δ*wA*, Δ*yA*, *veA1*, Δ*nkuA*, *pyrG89*) to allow for direct assessment of the transferred pigment biosynthetic clusters effect on the visual phenotype of the new host.

The individual gene clusters were transferred in their entirety to *A. nidulans* to simulate the situation following a HGT event (Figure 1). The transfer of DNA was performed using protoplast-mediated transformation and *in-vivo* homologous recombination based assembly of the introduced gene cluster fragments. A genomic locus of integration was chosen for which microarray data have previously shown constitutive expression (Andersen et al., 2013). Diagnostic PCR reactions, bridging the assembled fragments, verified successful fragment assembly and integration into the targeted locus (Supplementary Figure 2). The genome of the two PCR verfied strains were further analyzed by whole genome sequencing, using Illumina HiSeq at >150x coverage, with the aim of identifying mutations that the PCR-based transfer could have introduced. A focused SNP-analysis of the coding and intergenic regions of the transferred 17 kb bikaverin cluster showed that no mutations had been introduced. Analysis of the 25 kb aurofusarin cluster revealed a synonymous substitution in the GIP1 gene (K640) and a E280V mutation in AurJ. Targeted sequencing of these positions, neither of which were in the 1.5 kb overlapping regions of homology, in the *F. graminearum* PH1 donor showed that the mutations were introduced during PCR amplification. In a closer investigation of the E280V mutation, an alignment was made of the top 100 closest homologues of AurJ as identified by BlastP. The frequency distribution showed isoleucine as the most common residue in this position (55%), followed by V (25%) and E or T (both 10%) (Supplementary Figure 3). The effect of the E280V mutation in AurJ was therefore deemed limited. The strains containing the transferred bikaverin- or aurofusarin gene clusters were denoted *An_FfBIK* (IBT35518) and *An_FgAUR* (IBT35517) respectively. An overview of strains is presented in Table 1.

The bikaverin BGC sustains bikaverin production after HGT to *A. nidulans*

The *An_FfBIK* strain was cultivated on minimal and complex media to analyze for the production of bikaverin and known pathway intermediates (Table 2, structures shown in Supplementary Figure 4) that were expected to be produced if the bikaverin gene cluster was active after its transfer to *A. nidulans*.

Extracts of *An_FfBIK*, cultivated on solid or liquid YES medium for 7 days at 37 °C, were analysed by UHPLC-HRMS. This metabolomics analysis revealed production of the ultimate pathway product bikaverin (chromatograms can be seen in Supplementary Figure 5). While bikaverin production in *F. fujikuroi* is associated with a red phenotype (Wiemann *et al.*, 2009), there was no visible color change in the *A. nidulans* recipient strain, showing that the compound was produced at very low levels. In the corresponding UHPLC-HRMS based metabolite analysis, the signal intensity of bikaverin was low compared to that of the most abundant ion at the time of elution, as represented by the Base Peak Chromatogram (Supplementary Figure 5C). In contrast to the original host *F. fujikuroi*, the generated strain *An_FfBIK* did not produce detectable quantities of the intermediate nor-bikaverin (Wiemann *et al.*, 2009) or oxo-pre-bikaverin (Arndt *et al.*, 2015). The production of bikaverin was found to be media-dependent as no pathway-related products were detected in liquid or solid MM (Supplementary Figure 5).

Given that the bikaverin gene cluster was found to be active on YES medium after its transfer to *A. nidulans*, we next analyzed the metabolic profile via the unbiased chemical feature detection software Mass Profiler (Fischer, Steven M; Dai, 2015). The aim here was to screen for cross talk between bikaverin pathway metabolites and *A. nidulans* native enzymes, or bikaverin pathway enzymes and *A. nidulans* metabolites. While certain chemical features were more abundant in the *An_FfBIK* strain than in the *A. nidulans* reference strain, bikaverin was identified as the sole novel compound.

A. nidulans produces an aurofusarin pathway intermediate and dimeric shunt products, but not aurofusarin, after receiving the aurofusarin BGC

Cultivation of the *An_FgAUR* strain on solid YES medium resulted in the production of the monomeric pathway intermediate rubrofusarin (**7**) at low abundance. Neither dimeric 9-hydroxyrubrofusarin (**9**) nor aurofusarin (**10**) were detected (Figure 2A). The strain was found not to produce aurofusarin pathway-related metabolites in detectable amounts when cultured on solid MM, similar to the findings for the *An_FfBIK* strain cultured on MM.

Using the unbiased chemical feature detection approach, extracts of the *An_FgAUR* strain cultivated on YES medium were then screened for cross talk or shunt product formation. In addition to rubrofusarin, three unique masses were identified in *An_FgAUR,* suggesting the production of aurofusarin pathway related shunt products (Figure 2B). The first compound was found to have a monoisotopic mass of *m/z* 517.1130 Da equivalent to $C_{28}H_{20}O_{10}$ (**11**), and the masses of the last two features (**12.1**) and (**12.2**) matched that of the $[M+H]^+$ adduct of compounds with a molecular formula of $C_{29}H_{22}O_{10}$ (Figure 2C). The MS/MS spectra of (**12.1**) and (**12.2**) showed fragmentation resulting in the formation of (**6**) and (**7**) as product ions, suggesting that (**12.1**) and (**12.2**) are partially reduced heterodimers of (**6**) and (**7**) (Supplementary Figure 6). Similarly MS/MS analysis of compound (**11**) point towards it being a partially reduced homodimer of (**6**).

Expression of *aurR1* and activity of *aurF* are identified as pathway bottlenecks after aurofusarin BGC transfer to *A. nidulans*

Detection of the monomer (**6**) and dimers of (**6**) and (**7**) as shunt products in the strain *An_FgAUR* indicated functional expression of the genes encoding polyketide synthase PKS12, the dehydratase AurZ*,* the O-methyl transferase AurJ, as well as the laccase GIP1 and monooxygenase AurF required for dimerization and oxidation of (**7**) to (**8**) (Frandsen *et al.*, 2011). The accumulation of only partly oxidized dimers indicates that the oxidation step represents a pathway bottleneck in the new host, the cause of which we hypothesized to be a lack of transcriptional or enzymatic activity of AurF or GIP1.

RT-qPCR based expression analysis of the cluster genes in the *An_FgAUR* strain after 48h cultivation on YES medium did not shed light on this hypothesis, as it demonstrated transcription of all but one of the cluster genes (Supplementary Figure 7). The only gene for which no transcript was observed was *aurZ*, encoding the dehydratase AurZ that is required for the conversion of YWA1 to nor-rubrofusarin (Frandsen *et al.*, 2011). The primer pairs designed for the expression analysis spanned an intron where applicable, and further analysis showed that the targeted intron regions in the produced pre-mRNA's were spliced to yield the expected mature mRNAs. The evaluation of the enzymatic bottlenecks in the pathway thus continued by HPLC-MS based global proteomics analysis of the *An_FgAUR* strain, prepared after 48h of cultivation on YES medium in biological duplicates. The analysis allowed the identification of 4036 proteins with high confidence (Supplementary File 1) including eight out of ten aurofusarin pathway proteins, among which was AurZ. The membrane-bound transporter AurT and putative transcription factor AurR2 were not detected. The pathway specific transcription factor AurR1 was detected at very low levels, or not at all.

To investigate whether the lack of aurofusarin production could be attributed to insufficient levels of AurR1, AurF, or GIP1, additional copies of these genes, controlled by the strong *gpdA* promoter were introduced into the *An_FgAUR* strain in a separate locus, resulting in the strains *An_FgAUR*+OE:*aurR1*, *An_FgAUR*+OE:*aurF*, and *An_FgAUR*+OE:*gip1*. Overexpression of *aurF* or *gip1* did not lead to the production of aurofusarin, showing that neither of these enzymes were responsible for the bottleneck. The increased levels of AurF

or GIP1, however, resulted in increased abundance of the (**11**) and (**12**) dimers and a complete disappearance of monomeric rubrofusarin (**7**), compared to the *An_FgAUR* strain. Overexpression of the activator *aurR1* result in a boost of the levels of rubrofusarin (**7**) and the dimeric (**11**) and (**12**), and allowed for the production of aurofusarin (**10**) (Figure 3).

RT-qPCR demonstrated that the expression levels of all pathway genes was higher upon overexpression of aurR1 (in the *An_FgAUR*+OE:*aurR1* strain) compared to the *An_FgAUR* reference (Figure 4A). The strongest effects were observed for *aurR1* and the genes *gip1*, *aurF*, *aurC*, and *aurS* located downstream of the gene encoding PKS12. These findings were confirmed at the protein level by HPLC-MS, where the relative abundance difference before and after *aurR1* overexpression was greatest for AurR1 and AurZ-AurS (Figure 4B). Interestingly, detection of four unique frame-shift peptides from AurF in *An_FgAUR*+OE:*aurR1* indicated that the first intron in *aurF* was not always excised (Supplementary Figure 8).

Although the aurofusarin pathway was active after transfer to *A. nidulans*, the above data suggested that the absence of final pathway product aurofusarin was caused by low transcription of the pathway transcription factor aurR1, with the consequence of low abundance of all the necessary tailoring enzymes.

The transferred bikaverin and aurofusarin gene clusters are active even in the absence of the pathway specific transcription factors *bik5* and *aurR1*

In native hosts *F. fujikuroi* and *F. graminearum,* small amounts of bikaverin and aurofusarin are produced in absence of their respective pathway transcription factors *bik5* and *aurR1* (Frandsen *et al.*, 2006; Wiemann *et al.*, 2009), although visual pigmentation is lost (Kim *et al.*, 2006). To determine whether this persisted after horizontal transfer to *A. nidulans*, we generated strains with knockout of the respective transcription factors, *An_FgAURΔaurR1* and *An_FfBIKΔbik1* strains, and analyzed their metabolite profiles.

We found that the presence of a pathway-specific transcription factor was not essential for the production of pathway metabolites in *A. nidulans*. Production of rubrofusarin from the transferred aurofusarin cluster was sustained on YES medium after deletion of *aurR1*, and comparable amounts of the shunt products (**11**) and (**12**) were still observed (Figure 5A). Interestingly, rubrofusarin was detected in *An_FgAURΔaurR1* on MM even though it was not produced by the *An_FgAUR* strain with *aurR1* under the same conditions. In the case of the bikaverin cluster, we found that bikaverin was produced by *An_FfBIKΔbik5* on YES, albeit at 10-fold lower intensity than in the *An_FfBIK* strain (Figure 5B), suggesting a low basal transcription level of the cluster genes.

The bikaverin cluster shows a conserved transcriptional response to pH, but not to nitrogen after transfer to *A. nidulans*

In cases where a transferred BGC results in the production of the corresponding SecMets, the recipient organism does not necessarily experience an ecological advantage, particularly if this production is unresponsive to environmental cues. The compatibility of the BGC with the recipient organism's regulatory network is arguably equally important for the evolutionary success of the HGT event. Previous studies characterized the response of the bikaverin cluster to abiotic and biotic cues in the original host *F. fujikuroi* and the HGT recipient *B. cinerea* (Table 3). Responses to certain cues, such as exposure to the bacterial secondary metabolite ralsolamycin, were conserved in *F. fujikuroi* and *B. cinerea*, while the response to nitrogen levels was reversed (Spraker *et al.*, 2018). This formed the starting point for investigating the transcriptional response of the bikaverin gene cluster to environmental cues

after its transfer to *A. nidulans*. For this, the *An_FfBIK* strain was cultured on solid YES medium at 37 °C, and analyzed after 48 and 72 h. The transcriptional level of the cluster was found to be higher at 48 h than 72 h (data not shown), matching the 48 h expression peak reported in *F. fujikuroi* (Wiemann *et al.*, 2009). Subsequent experiments were conducted with a 48 h sampling time.

We first assessed the transcriptional response to nitrogen availability by cultivating *An_FfBIK* on solid defined medium containing 6 mM or 60 mM NH_4NO_3. While high nitrogen levels repress the bikaverin cluster in *F. fujikuroi* and *B. cinerea*, the transferred bikaverin cluster and its adjacent genes were not differently expressed in *A. nidulans* under the two conditions studied (Supplementary Figure 9). On the contrary, the response of the bikaverin cluster in *An_FfBIK* to environmental pH followed the regulation observed in *F. fujikuroi*. Expression of *bik3*, *bik4*, and *bik6* was significantly higher during cultivation on YES medium buffered at pH 4 compared to pH 8 (Figure 6A).

The fungal pH regulatory system, based on the regulatory protein PacC and its recognition consensus sequence *5'-GCCARG-3'*, was discovered in *A. nidulans* (Espeso *et al.*, 1997; Valkonen *et al.*, 2002) and is widely conserved across many fungal genera including *Fusaria* (Caracuel *et al.*, 2003), Penicillia (Suárez and Peñalva, 1996) and *Magnaporthe* (Landraud *et al.*, 2013). Wiemann et al. found that PacC mediates repression of the bikaverin cluster at high pH in *F. fujikuroi* (Wiemann *et al.*, 2009). There are PacC recognition sites in the promoter regions of *bik1* (71, 86, 157 nt upstream of ATG), *bik5* (66 nt upstream of ATG), and *bik4* (370 nt upstream of ATG), and based on the high degree of conservation of the PacC regulatory system, we hypothesized that *PacC* orchestrates the observed pH response in *A. nidulans*, as it does in *F. fujikuroi*. Indeed, the significant repression of *bik3*, *bik4*, and *bik6* at high pH disappeared upon deletion of the endogenous pacC, and was even reversed in the case of *bik4* (Figure 6A). Comparison of transcript levels between the *An_FfBIK* strain and the *pacC* deletion mutant *An_FfBIKΔpacC* confirmed that the *A. nidulans* PacC is able to control the *F. fujikuroi* bikaverin cluster (Figure 6B). Transcription of all *bik* genes in *An_FfBIKΔpacC* was significantly higher at pH 8, reflecting that PacC is proteolytically activated at high pH (Espeso and Arst, 2000; Bussink *et al.*, 2015). Although the cluster is repressed by PacC, deletion of *pacC* did not result in bikaverin production on MM.

The bacterial metabolite ralsolamycin does not specifically induce expression of the bikaverin cluster in *A. nidulans*

In addition to protecting a fungus from abiotic stressors, SecMets can form effective defensive or offensive strategies in inter-species interactions, an intricate example of which is the interaction between various fungi and the bacteria *R. solanacearum* (Keller, 2019). *F. fujikuroi, B. cinerea* and *A. nidulans* were among 34 fungal species that formed thick-walled survival structures reminiscent of chlamydospores as a response to exposure to ralsolamycin, a diffusible SecMet produced by the hybrid non-ribosomal peptide synthase / polyketide synthase RmyA in *Ralstonia solanacearum* (Spraker *et al.*, 2016). A recent follow-up study found that, in addition to cellular differentiation, exposure to *R. solanacearum* culture extracts containing ralsolamycin induced production of bikaverin in both *F. fujikuroi* and *B. cinerea*, even overriding the nitrogen response (Spraker *et al.*, 2018). Having characterized the transcriptional response of bikaverin genes in the *An_FfBIK* strain to two abiotic factors, we asked if the bikaverin cluster retained its response to ralsolamycin.

Upon exposure to extracts of wild type *R. solanacearum* GMI1000, but not extracts of the Δ*rmyA* mutant, we observed formation of chlamydospore-like structures in liquid cultures of the *An_FgAUR* strain and *F. fujikuroi* (Supplementary Figure 10). Unlike *B. cinerea* or *F.*

fujikuroi, the *An_FgAUR* strain did not form an inhibition zone when culture supernatant of *R. solanacearum* GMI1000 was spotted at 1 cm distance on solid YES medium, buffered at pH 4 or pH 8 (data not shown). RT-qPCR analysis of bikaverin gene expression in the interaction zone at either pH did not show a strong response of bikaverin genes to ralsolamycin in *An_FfBIK* (Figure 6B and C).

Discussion

The HGT of biosynthetic gene clusters is an important contributor to evolution of secondary metabolism in fungi. However, due to a paucity of experimental work we lack understanding of the functional implications of acquiring a new gene cluster, which influences the evolutionary fate of the transferred cluster. Our findings of the experimental transfer of the bikaverin and aurofusarin gene clusters highlight how transcript levels influence which products are formed from an acquired cluster, and how the presence of cis-regulatory elements could help to co-transfer regulatory mechanisms along with transfer of genes.

Transfer of the aurofusarin cluster as a model for how HGT can shift pathway bottlenecks and lead to the formation of novel shunt products

Transcriptional activation is the first challenge that horizontally transferred genes encounter once they have been integrated in their new genomic context. Size seems to matter, low transcription levels being one of the disadvantages faced by longer transferred sequences (Husnik and McCutcheon, 2018). In the current study, production of pathway products indicated that the aurofusarin and bikaverin clusters overcame this challenge after transfer when cultivated on a complex medium (Supplementary Figure 5, and Figure 2). Pathway metabolites were even produced at low levels in absence of the pathway specific transcription factors *aurR1* and *bik5* (Figure 5), perhaps as a result of the selected *A. nidulans* locus. However, no cluster products were detected from either cluster on minimal medium. Even on complex medium, the production of bikaverin by *A. nidulans* was not sufficient to result in the red phenotype that is associated with expression of the bikaverin cluster in the natural host *F. fujikuroi* (Wiemann *et al.*, 2009). Moreover, the aurofusarin cluster did not result in aurofusarin production at all: *An_FgAUR* instead produced rubrofusarin and dimeric shunt products (**11**) and (**12**) (Figure 2), which have not been reported in *F. graminearum* wild type or with *aurR1* overexpression (Westphal *et al.*, 2018). At the low observed level of activity, the clusters may not have a strong fitness effect in early generations of the new host. While Berg and Kurland proposed strong positive selection to be necessary for transferred genes to become fixed in a population (Berg and Kurland, 2002), another study calculated that neutral or slightly deleterious genes can also become fixed in a bacterial population (Novozhilov *et al.*, 2005). After fixation, the transferred cluster could face a range of evolutionary fates depending on the biological activity of its gene products and pathway metabolites, and their combined fitness effects in the given genomic and environmental context.

Production of rubrofusarin and new shunt products, rather than aurofusarin, pointed to a shift in the pathway bottleneck after HGT of the aurofusarin cluster. Closer investigation linked the molecular formulae of the detected masses (**11**) and (**12**) to a possible lack of monooxygenase activity by AurF, and later detection of a frame shift peptide product from AurF indicated that the first intron of *aurF* was not spliced as expected from a portion of the transcripts originating from the gene (Supplementary Figure 8). However, overexpression of *aurF* or *gip1* did not result in aurofusarin production. Meanwhile, low abundance of the transcription factor AurR1 protein in the proteomics analysis raised the possibility of low transcriptional activation of the cluster (Figure 4). Boosting AurR1 activity through overexpression under the *gpdA* promoter strongly upregulated *aurF* as well as the genes *aurJ*, *gip1*, and *aurS* (Figure 4), similar to what was described in *F. graminearum* (Westphal

et al., 2018). Consequently, overexpression of *aurR1* in *A. nidulans* resulted in the production of aurofusarin in addition to shunt products (**11**) and (**12**) (Figure 3). Overexpression of *aurR1* therefore partially resolved the pathway bottleneck in a way that overexpression of *aurF* or *gip1* alone did not. A possible explanation for this could come from the earlier theory that AurF interacts with AurO, GIP1 and AurS to form a protein complex necessary for aurofusarin formation (Frandsen *et al.*, 2011).

Central to discussing the barriers after HGT is the ”complexity barrier” hypothesis, which states that genes with a high degree of connectivity to regulatory systems or protein-protein interactions have a lower chance of undergoing a successful HGT (Jain *et al.*, 1999; Jain *et al.*, 2002). This is particularly relevant if the product of a transferred gene forms part of a protein complex with host subunits (Wellner and Gophna, 2008). Although AurF was suggested to be part of a protein complex (Frandsen *et al.*, 2011), the interacting subunits in the putative complex are encoded by co-transferred genes. Following the selfish operon theory, the aurofusarin cluster thus forms an independent evolutionary unit (Lawrence, 1999; Lawrence, 2003). What this fails to take into account, however, is that the fine-tuning of transcript levels necessary to form a functional complex likely occurs over millions of years (Lercher and Pál, 2007) and that this transcriptional fine-tuning is not likely to be transferred precisely to a new host. Low transcription could result in failure to form a functional complex (Deutschbauer *et al.*, 2005), while a stoichiometric imbalance of the subunits may be detrimental to activity of the protein complex (Papp *et al.*, 2003; Veitia, 2004). If tailoring enzymes of the aurofusarin pathway indeed form a protein complex as previously suggested (Frandsen *et al.*, 2011), then perhaps a lack of transcriptional fine-tuning after the simulated HGT event resulted in suboptimal functioning of this complex, leading to accumulation of rubrofusarin and the formation of novel shunt products.

Fine-tuning a biochemical pathway in its original host does not mean all intermediates are immediately and solely converted to one final product. In *F. graminearum*, for example, the ratio of rubrofusarin to aurofusarin ranged between 2:1 to 3:1 over the course of nine days (Frandsen *et al.*, 2011). Cross talk frequently occurs on multiple levels, including between metabolites and gene clusters, and in interactions with primary metabolism and homeostasis (Sheridan *et al.*, 2015). As an example of this, the aurofusarin pathway in *F. graminearum* is redirected to produce citreoisocoumarin and SMA93, respectively, under low nitrogen or low pH conditions (Sørensen *et al.*, 2012). This redirection was not observed in *A. nidulans*. It must be noted here that the the most likely interaction partners for the transferred aurofusarin cluster, *A. nidulans* pigmentation genes *wA* and *yA*, were absent in the pigment-deficient strain of *A. nidulans* that was used as the recipient in this study. *A. nidulans* wA and *F. graminearum* PKS12 both catalyze formation of YWA1 (Watanabe *et al.*, 1999; Frandsen *et al.*, 2011). In *A. nidulans*, the laccase yA polymerizes YWA1 to produce green conidial pigmentation (Clutterbuck, 1972), while YWA1 is the first intermediate of the aurofusarin pathway in *F. graminearum*. Transfer of the aurofusarin BGC to wild type *A. nidulans* may result in cross talk between these two pathways, influencing the product spectrum. Whether cross talk or a new bottleneck, arising from low or imbalanced transcription after HGT, is deleterious or beneficial depends on the biological properties of the metabolites as well as the selective pressures experienced by the recipient strain.

Factors that determine the conservation of regulation after HGT

The aurofusarin and bikaverin gene clusters were integrated in a region of the *A. nidulans* chromosome known for high transcription. Bikaverin was immediately produced after transfer, while a further boost of cluster-specific transcript levels was necessary for *A. nidulans* to produce aurofusarin. However, higher transcription does not necessarily increase the chance of fixation of transferred genes. In fact, high transcription was found to be the single biggest determinant of HGT failure in bacteria (Park and Zhang, 2012). Regulation following HGT is crucially important for the evolutionary fate of the transfer event, yet understudied in the context of fungal secondary metabolism. We therefore characterized the response of the bikaverin cluster to various environmental cues and compared the observed

responses to those in natural hosts *F. fujikuroi* and *B. cinerea* (Table 3), aiming to understand which regulatory mechanisms facilitate the conservation of regulation after HGT of a SecMet gene cluster.

When subjecting *An_FfBIK* to changing nitrogen availability, environmental pH, and exposure to bacterial SecMet ralsolamycin, only the pH response of *bik* genes was found to be conserved after cluster transfer from *F. fujikuroi* to *A. nidulans* (Table 3). The expression of all *bik* genes was higher at low pH*,* with significant differences for *bik3*, *bik4*, and *bik6* (Figure 6A). Moreover, transcription of all *bik* genes was significantly higher at pH 8 after deletion of the high-level fungal transcription factor encoding gene *pacC* (Figure 6B). Despite PacC being proteolytically activated at high pH, the derepression effect persisted at pH 4, though less strongly than at pH 8. While mutating PacC recognition sites rather than deleting *pacC* would refine findings by limiting pleiotropic effects, these results closely follow the findings of Wiemann et al. in *F. fujikuroi* (Wiemann *et al.*, 2009). In the transfer of the bikaverin cluster, PacC plays an essential role in conserving the pH response after HGT.

The role of PacC in the horizontal transfer of the bikaverin cluster forms an example of how cis-regulatory elements and their recognition by a conserved regulatory protein facilitate the conservation of regulatory cues after HGT. The response may initially be weaker as the binding site is not optimal for the regulatory protein in the new host, but this can improve over time as cis-regulatory elements of horizontally transferred genes show accelerated evolution (Lercher and Pál, 2007). Further investigation could extend to characterizing the pH response of the aurofusarin cluster. Aurofusarin is not produced in *F. graminearum* below pH 4 (Medentsev *et al.*, 2005), with PacC binding sites located 124 nt and 43 nt upstream of *aurR1* and *aurS*, respectively, suggesting involvement of PacC. Moreover, transferring the bikaverin cluster across larger phylogenetic distances could indicate the limits of the conserved pH response, as recognition of cis-regulatory elements is inversely related to phylogenetic distance (Gasch *et al.*, 2004). This would also test the hypothesis posited by Clevenger et al. (Clevenger *et al.*, 2017), that pro-repressive elements are more likely to be effective in more closely related species. Opposite to conservative cis- regulation, horizontal transfer over large phylogenetic distances could also lead to birth of new cis-regulatory elements, as was shown after the transfer of a cellulose synthase gene from bacteria to tunicates (Sasakura *et al.*, 2016). The acquired DNA contained GC-rich regions that acted as a recognition site for the transcription factor AP-2, which enabled tissue-specific expression and resulting production of cellulose, a defining characteristic of tunicates.

Contrary to PacC-mediation of the pH response, the GATA transcription factor AreA does not mediate a nitrogen response of *bik* genes in *F. fujikuroi* (Wiemann *et al.*, 2009). While strong nitrogen repression was observed in *F. fujikuroi*, *bik* genes were induced by nitrogen in *B. cinerea* and became unresponsive to nitrogen levels when in *A. nidulans* (Table 3). We hypothesize that the nitrogen response of the *bik* cluster, in absence of recognized cis-regulatory elements, depends on the chromosomal context, and is therefore less likely to be conserved after HGT. This hypothesis extends to regulation by chromatin remodeling: whether or not such regulation is conserved after HGT is predicted to depend on the locus of integration. Exemplary is regulation by the velvet complex, in which light-induced Vel1/VelA is complexed with sexual development regulator VelB and chromatin remodeling protein LaeA (Bayram *et al.*, 2008). Although conserved across diverse fungi, its role is diverse (Bayram and Braus, 2012), and many genes that are regulated by VelA in one species are independent of VelA in another species (Lind *et al.*, 2015). In case of the bikaverin cluster, Vel1 showed opposite regulation of *bik* genes in *F. fujikuroi* compared to HGT recipient *B. cinerea*, independent of which Vel1 homologue (FfVel1 or BcVel1) was present in the strains (Schumacher *et al.*, 2013). Location specificity was shown directly for VelA interaction partner LaeA in *A. nidulans*; the primary metabolic gene *argB* experienced the same LaeA-mediated silencing as the sterigmatocystin cluster when placed in its locus (Bok *et al.*, 2006).

The regulatory mechanism behind the interaction between the bikaverin cluster and the bacterial SecMet ralsolamycin forms another interesting and hitherto unresolved question. In both *F. fujikuroi* and *B. cinerea*, ralsolamycin upregulates *bik* genes (Spraker *et al.*, 2018). Is

the response of the bikaverin cluster in *F. fujikuroi* mediated by a specific cis-regulatory element within- or close to the gene cluster, as recently hypothesized (Keller, 2019)? Under the conditions tested, the current study did not find evidence that ralsolamycin exposure induces expression of the bikaverin cluster after its transfer to *A. nidulans*. However, we did confirm that ralsolamycin induces the formation of chlamydospore-like structures in *F. fujikuroi* and *A. nidulans*, as was previously reported for these and 32 other fungal species (Spraker *et al.*, 2016). We therefore propose that the ralsolamcyin-induced upregulation of the bikaverin cluster in *F. fujikuroi* is a fortunate pleiotropic effect (ie. chromatin remodeling) of the chlamydospore response, rather than the result of a cis-regulatory element within the bikaverin cluster. Further investigation could determine whether the bikaverin induction in response to ralsolamycin persists when the bikaverin cluster is transferred to different loci in *F. fujikuroi*, and in other fungal species that contain the bikaverin cluster.

Even though the DNA transfer mechanism by which HGT of fungal BGCs occurs in nature is yet to be understood, the presented experimental strategy offers an opportunity to study the aftermath of such events. The current study demonstrates that experimentally simulating HGT events using well-characterized model systems can form a powerful tool in deepening our understanding of the functional consequences of HGT. We find that novel metabolites can arise after HGT, and identify gene regulation as an important influence on the effect of a transferred cluster in its new genomic context. We posit that the field of fungal secondary metabolism will benefit from expanding *in silico* HGT studies with interdisciplinary empirical work, including comparative transcriptomics and organism interaction studies in addition to experimental transfer of gene clusters.

Experimental Procedures

Strains and media

Plasmids were constructed by USER cloning (Nour-Eldin *et al.*, 2006; Hansen *et al.*, 2011) and propagated in *Escherichia coli* DH5α using 100 µg mL^{-1} ampicillin as selection on solid or liquid LB medium. Oligonucleotides used in the study were purchased from TAG Copenhagen and are listed in Supplementary Table 1.

Fungal strains were generated starting from a pigment-deficient *A. nidulans* mutant IBT35516
(Δ*wA*, Δ*yA*, *veA1*, *pyrG89,* Δ*nkuA*) (Holm, 2013), derived by deletion of *wA* and *yA* from parent strain IBT29539 (*argB2, pyrG89, veA1, nkuA*Δ) (Nielsen *et al.*, 2008), and available from the IBT Culture Collection at the Department of Biotechnology and Biomedicine, Technical University of Denmark, Denmark. For generation of subsequent *A. nidulans* strains, protoplasts were generated and transformed as described by Nielsen et al. (Nielsen *et al.*, 2006), using the *Aspergillus fumigatus* PyrG (*AfpyrG*) selection marker. Unless stated otherwise, strain verification was performed using MyTaq Plant-PCR kit (Bioline BIO-25055). An overview of the strains constructed and used in this study is shown in Table 1.

Fungal strains were cultivated on liquid or solid (2 % agar) media. Yeast extract sucrose (YES) medium at pH 6.5 contained 2 % yeast extract (Biokar A1202HA), 15 % sucrose, 0.05 % $MgSO_4 \cdot 7H_2O$ in addition to 1x Cove's Trace Elements (Cove, 2015). Minimal medium (MM) at pH 6.5 was made according to (Kaminskyj, 2001), using 1x Cove's Trace Elements. For transformations, glucose was substituted with 1 M sucrose. Media were supplemented with 10 mM uridine (Uri) and 10 mM uracil (Ura) where necessary. Curing of the PyrG selection marker was performed using 5-fluoroorotic acid (5-FOA) on MM supplemented with Uri and Ura. For high- and low- nitrogen medium, $NaNO_3$ in MM was substituted for either 6mM or 60 mM NH_4NO_3 as sole nitrogen source. YES medium was buffered at high- or low-pH with 0.2 M acetate buffer (pH 4) or phosphate buffer (pH 8), added to a final

concentration of 50 mM. For testing chlamydospore formation, strains were grown in liquid 10 % or 100 % ICI medium (Spraker *et al.*, 2018).

Transfer of the aurofusarin and bikaverin gene clusters, and strain verification

The bikaverin and aurofusarin gene clusters were transferred to recipient strain IBT35516 using *in-vivo* homologous recombination (Figure 1). First, the clusters including 1kb flanking regions were amplified in 8-10 kb fragments with 1.5 kb overlapping regions from donor genomes *Fusarium fujikuroi* IMI58289 (Huß *et al.*, 2013) and *Fusarium graminearum* PH-1 / ATCC MYA-4620 / FGSC 9075 / NRRL 31084 , sequenced by King et al 2015 (King *et al.*, 2015). PCR amplification was conducted using Phusion High-Fidelity polymerase (Thermo Fisher Scientific) and reactions were scaled up to obtain 2 μg of each fragment. Fragments were purified using the GenElute PCR clean-up kit (Sigma Aldrich) and concentrated by ethanol precipitation (Green and Sambrook, 2016). Next, 1.5 kb up- and down- flanking regions of the cluster ($UF_{cluster}$ and $DF_{cluster}$) were amplified and cloned into targeting construct pU2005-5 (Hansen *et al.*, 2011), containing 1.5 kb homologous sequences up- and downstream of the selected integration locus in *Aspergillus nidulans* ($USTS_{A.nid}$ and $DSTS_{A.nid}$) and the *AfpyrG* selection marker, with intermediary SwaI restriction sites. This resulted in plasmid pER1 for the aurofusarin cluster and pER2 for the bikaverin cluster. The targeting fragments $USTS_{A.nid}$-$UF_{cluster}$ and $DF_{cluster}$-*AfpyrG*-$DSTS_{A.nid}$ were then released from pER1 and pER 2 by digestion with SwaI (New England Biolabs) and gel purified. Third, between 1-2 μg of each cluster fragment was added directly to the transformation mix alongside 0.5 μg of the SwaI-digested targeting construct pER. Finally, genomic DNA was purified from transformants via the FastDNA SPIN kit for Soil DNA (MP Biomedicals) and *in-vivo* homologous recombination of the cluster in the correct locus was verified by diagnostic PCR. Absence of deleterious SNPs was confirmed by Illumina HiSeq2500 high-coverage whole-genome sequencing and variant calling (executed by BaseClear, NL).

Metabolite profiling by Ultra High Liquid Chromatography – High Resolution Mass Spectrometry (UHPLC-HRMS/MS)

Biomass was harvested as 3 x 0.6 cm^2 plugs from solid medium, or a similar biomass amount from liquid culture. Metabolites were extracted in 1 mL 1:3 ethyl acetate/isopropanol (v/v) with 1% formic acid using 1 h ultra sonication, after which the extraction solvent was evaporated and metabolites resuspended in 300 μL HPLC grade methanol. Compounds were separated in an Agilent 1290 Infinity UHPLC (Agilent Technologies) equipped with an Agilent Poroshell 120 Phenyl Hexyl column (Agilent Technologies). The solvent system consisted of water and acetonitrile, both buffered with 20 mM formic acid, using a linear gradient increasing from 10% to 100% acetonitrile for 15 min, sustained for 2 min, returning to 10% acetonitrile in 0.1 min, ending with 10% acetonitrile for 3 min (flow rate 0.35 mL min^{-1}, column temperature 60 °) (Klitgaard *et al.*, 2014). Mass spectra were obtained on an Agilent 6545 QTOF MS with Agilent Dual Jet Stream electrospray ion source (Agilent Technologies). Drying gas was at a temperature of 250 °C and flow rate of 8 L min^{-1}, sheath at 300 °C and 12 L min^{-1}. Scan range was *m/z* 85–1700 in MS mode and *m/z* 30–1700 in MS/MS mode.

Data was analyzed in MassHunter Qualitative Analysis B.07.00 (Agilent Technologies), and compounds verified by manual dereplication (Klitgaard *et al.*, 2014; Nielsen and Larsen, 2015). Aurofusarin was further confirmed by comparison of MS/MS profile standard from in-house collection (Larsen *et al.*, 2011). The MS/MS spectra obtained for bikaverin were verified against those reported by Busman et al. (Busman *et al.*, 2012). IBT35516 was transformed with an empty targeting cassette containing the *AfpyrG* selection marker and used as reference strain for metabolite analyses.

Mass Profiler (Version B.07.01, Agilent Technologies) was used for unbiased feature detection (Fischer, Steven M; Dai, 2015). Ion intensity cut-off was set to 5000 count, RT tolerance to 1% and mass tolerance to 15 ppm. Comparison was performed using mass spectra of triplicate samples, taken from individual colonies in the each cultivation.

RT-qPCR expression analysis

Gene expression was measured in cultures on solid media. A 5 µL volume containing 1000 spores was inoculated on solid media and cultivated for 48 h or 72 h at 37 °C. A pie slice of the colony, ranging from the colony center to its periphery and with an approximate surface area of 1-2 cm^2, was carefully excised and transferred to a 2 mL Eppendorf micro centrifuge tube containing a 4 mm metal bead. Samples were frozen in liquid nitrogen for immediate use or storage at -80 °C. Biomass was disrupted at 50 MHz for 50 s in TissueLyzer LT (Qiagen) with a sample holder cooled to -20 °C. RNA was extracted and purified, following manufacturer's instructions including a gDNA spin column removal step, using RNA Easy Plus Mini Kit (Qiagen). Enzymatic DNAse treatment and cDNA synthesis were performed with QuantiTect Reverse Transcription Kit (Qiagen). RT-qPCR was performed with QuantiTect SYBR Green PCR Kit (Qiagen) in a CFX Connect thermal cycler (Bio-Rad) with a cycling program of 95 °C for 5 min, followed by 40 cycles of 95 °C for 10 s and 60 °C for 30 s, ending with a melting curve from 65 °C to 95 °C (0.5 °C increment per 5 s). Efficiencies of primer pairs were 90-110 % and absence of gDNA was verified on a sample of untranscribed RNA, and confirmed by analysis of primer melting curves. Histone H2A (AN3468) was used as reference gene (Andersen *et al.*, 2013). Relative expression levels of condition A versus condition B were calculated as the $\log_2$fold change $\Delta\Delta C(t)$, with $\Delta\Delta C(t) = \Delta C(t)_{conditionA} - \Delta C(t)_{conditionB}$, where $\Delta C(t)_{conditionN} = \Delta C(t)_{H2A,conditionN} - \Delta C(t)_{target\ gene,conditionN}$.

The interaction with ralsolamycin was measured with supernatants of *Ralstonia solanacearum* GMI1000 or Δ*rmyA* cultivated in CPG medium, and a CPG medium blank, according to Spraker et al. (Spraker *et al.*, 2018). Extracts were kindly provided by the Keller Lab (University of Wisconsin–Madison, WI, USA). Following inoculation of *A. nidulans* as described above, 5 µL of supernatant was spotted at 1 cm distance from the inoculation point. Biomass was excised in a pie-shaped fragment centered around the supernatant spot, and RT-qPCR performed as described.

Proteomics by HPLC-MS

For global proteome analysis, biomass was harvested from solid media, frozen in liquid nitrogen, and pulverized in TissueLyzer LT as previously described for RT-qPCR. Lysis, digestion and desalting was performed following Kulak et al. (Kulak *et al.*, 2014). Briefly, the pulverized biomass was mixed with 10 volumes of lysis buffer (6M Guanidinium Hydrochloride, 10 mM TCEP, 40 mM CAA, 50 mM HEPES, pH 8.5) and transferred to a Protein LoBind micro centrifuge tube (Eppendorf). The sample was boiled for 5 min, cooled on ice, and 100 µL transferred to a new tube for 5 sonication cycles (15 s ON, 10 s OFF) at Max setting in BioRuptor (Diagenode). The sample was centrifuged 10 min at 4 °C, supernatant transferred to a clean tube, and protein concentration determined using Bradford (Sigma-Aldrich). An equivalent of 50 µg protein was diluted 1:3 with digestion buffer (10% Acetonitrile, 50 mM HEPES pH 8.5) containing LysC (MS grade, Wako) at a 1:50 (enzyme to protein) ratio. Samples were incubated at 37 °C for 4 h, then diluted 1:10 with digestion buffer containing trypsin (MS grade, Promega) at a 1:100 (enzyme to protein) ratio and incubated at 37 °C overnight. Enzyme activity was quenched by adding 2 % trifluoroacetic acid (TFA) to a final concentration of 1%. Each sample was desalted on in-house packed C18 StageTips, consisting of two C18 discs (3M Empore) packed in a 200 µL pipet tip. The C18 material was activated with 40 µL 100% methanol (HPLC grade, Sigma), followed by 40 µL Buffer B (80% acetonitrile, 1 % formic acid). Tips were equilibrated with

two times 40 µL Buffer A' (1% TFA, 3% acetonitrile). Samples were loaded by centrifugation at 1800 G, washed twice with 100 µL formic acid, and eluted into clean tubes with 40% acetonitrile, 0.1% formic acid. Eluted peptides were concentrated in a SpeedVac (Eppendorf) and reconstituted in 1% TFA for further analysis.

Peptides were loaded onto a 2 cm C18 trap column (Thermo Fisher Scientific 164705) using 100% buffer A (0.1% formic acid in water). Separation was performed using the Thermo EasyLC 1000 HPLC system (Thermo Fisher Scientific) in single-column setup, equipped with a 50 cm C18 Thermo EasySpray reverse-phase analytical column (Thermo Fisher Scientific ES803), operated at 750 bar and 45 °C. Peptides were eluted in a linear gradient from 6% to 60% buffer B (80% acetonitrile, 0.1% formic acid) using a flow rate 0.25 mL min^{-1}. Mass spectra were obtained on a Q-Exactive (Thermo Fisher Scientific) run with a DD-MS2 top10 method. MS spectra were collected at a resolution of 70,000, with an AGC target of 3 x 10^6 or maximum injection time of 20 ms, scan range m/z 300-1750. MS/MS spectra were obtained at resolution of 17,500, with an AGC target of 3 x 10^6 or maximum injection time of 60 ms, normalized collision energy of 25 and intensity threshold of 1.7 x 10^4. Dynamic exclusion was set to 60 s, and ions with a charge state below 2 were excluded. Complex cell lysate quality control standards were used to verify performance consistency.

Raw files were analyzed for protein abundance using Proteome Discover 2.2 (Thermo Fisher Scientific) and its Minor Feature Detector for Label-free quantitation (LFQ). Spectra were matched against the *A. nidulans* protein reference database obtained from the *Aspergillus* Genome Database (*Asp*GD), expanded with bikaverin and aurofusarin protein sequences, in addition to translation products in six reading frames of unspliced mRNA from bikaverin and aurofusarin BGC genes. Oxidation (M), deamination (N, Q) and N-terminal acetyl were set as dynamic modifications. Results were filtered for 1% false discovery rate.

Control experiment for chlamydospore induction

An_FfBIK was cultivated as 3-point stab on solid MM for 4 days at 37 °C. Spores were harvested in 3 mL spore harvesting solution (0.9 % NaCl, 0.05 % Tween-80). *Fusarium fujikuroi* (IBT#41985) was cultivated on solid YPD for 4 days at 28 °C. Baffled 300 mL flasks containing 100 mL Darken medium (Darken *et al.*, 1959) were inoculated with 1 mL of *An_FfBIK* spore solution or 3 x 1 cm^2 plugs of *F. fujikuroi*. After 3 days incubation at 28 °C with 180 rpm shaking, 250 µL of the starter culture was used to inoculate 12 mL ICI medium (10% or 100%) in 50 mL culture tubes. Four mL of GMI1000- or Δ*rmyA* supernatant or CPG medium blank (as described previously) were added, and cultures were incubated at 28 °C, 180 rpm. Cultures were examined for chlamydospore formation and photographed after 3 days.

Acknowledgements

ER and RF acknowledge funding from the Danish National Research Foundation, grant number DFF-4181-00378, and grant number DNRF137 for the Center for Microbial Secondary Metabolites. We thank Nancy Keller and Nandhitha Venkatesh (Department of Medical Microbiology and
Immunology, Department of Bacteriology, University of Wisconsin–Madison, Madison, WI, USA) for generously providing extracts of *R. solanacearum G1000* and Δ*rmyA*, and are grateful for help of Erwin Schoof and Lene Holberg Blicher (DTU proteomics core, DTU Bioengineering, Technical University of Denmark, Lyngby, DK) in HPLC-MS analysis of the *An_FgAUR* proteome. We also Maria Maric (DTU Bioengineering, Technical University of Denmark, Lyngby, DK) for preliminary expression studies of the bikaverin cluster in *An_FfBIK*.

Author contributions

ER and RF conceived and designed the study. ER collected and analyzed data. MRN performed a proof of concept study for cluster transfer. ER and RF wrote and revised the manuscript. The final manuscript is approved by all authors.

Data availability statement

The data that support the findings of this study are available from the corresponding author upon reasonable request.

References

Andersen, M.R., Nielsen, J.B., Klitgaard, A., Petersen, L.M., Zachariasen, M., Hansen, T.J., *et al.* (2013) Accurate prediction of secondary metabolite gene clusters in filamentous fungi. *Proc Natl Acad Sci* **110**: E99–E107 http://www.pnas.org/cgi/doi/10.1073/pnas.1205532110.

Arndt, B., Studt, L., Wiemann, P., Osmanov, H., Kleigrewe, K., Köhler, J., *et al.* (2015) Genetic engineering, high resolution mass spectrometry and nuclear magnetic resonance spectroscopy elucidate the bikaverin biosynthetic pathway in Fusarium fujikuroi. *Fungal Genet Biol* **84**: 26–36 http://dx.doi.org/10.1016/j.fgb.2015.09.006.

Bayram, Ö., and Braus, G.H. (2012) Coordination of secondary metabolism and development in fungi: the velvet family of regulatory proteins. *FEMS Microbiol Rev* **36**: 1–24 https://academic.oup.com/femsre/article-lookup/doi/10.1111/j.1574-6976.2011.00285.x. Accessed November 8, 2018.

Bayram, O., Krappmann, S., Ni, M., Bok, J.W., Helmstaedt, K., Valerius, O., *et al.* (2008) VelB/VeA/LaeA complex coordinates light signal with fungal development and secondary metabolism. *Science* **320**: 1504–6 http://www.ncbi.nlm.nih.gov/pubmed/18556559. Accessed November 8, 2018.

Berg, O.G., and Kurland, C.G. (2002) Evolution of microbial genomes: Sequence acquisition and loss. *Mol Biol Evol* **19**: 2265–2276 http://academic.oup.com/mbe/article/19/12/2265/997594. Accessed February 18, 2019.

Bode, H.B., Bethe, B., Hofs, R., and Zeeck, A. (2002) Big Effects from Small Changes : Possible Ways to Explore Nature ' s Chemical Diversity. *ChemBioChem* **3**: 619–627.

Bok, J.W., Noordermeer, D., Kale, S.P., and Keller, N.P. (2006) Secondary metabolic gene cluster silencing in Aspergillus nidulans. *Mol Microbiol* **61**: 1636–1645 http://doi.wiley.com/10.1111/j.1365-2958.2006.05330.x. Accessed November 8, 2018.

Bonham, K.S., Wolfe, B.E., and Dutton, R.J. (2017) Extensive horizontal gene transfer in cheese-associated bacteria. *Elife* **6** http://www.ncbi.nlm.nih.gov/pubmed/28644126. Accessed June 13, 2018.

Brakhage, A. a., and Schroeckh, V. (2011) Fungal secondary metabolites - Strategies to activate silent gene clusters. *Fungal Genet Biol* **48**: 15–22 http://dx.doi.org/10.1016/j.fgb.2010.04.004.

Brown, D.W., and Proctor, R.H. (2016) Insights into natural products biosynthesis from analysis of 490 polyketide synthases from Fusarium. *Fungal Genet Biol* **89**: 37–51 http://linkinghub.elsevier.com/retrieve/pii/S108718451630007X.

Busman, M., Butchko, R.A.E., and Proctor, R.H. (2012) LC-MS/MS method for the determination of the fungal pigment bikaverin in maize kernels as an indicator of ear rot. *Food Addit Contam - Part A Chem Anal Control Expo Risk Assess* **29**: 1736–1742 http://www.tandfonline.com/doi/abs/10.1080/19440049.2012.704528. Accessed February

12, 2019.

Bussink, H.J., Bignell, E.M., Múnera-Huertas, T., Lucena-Agell, D., Scazzocchio, C., Espeso, E.A., *et al.* (2015) Refining the pH response in Aspergillus nidulans: A modulatory triad involving PacX, a novel zinc binuclear cluster protein. *Mol Microbiol* **98**: 1051–1072 http://www.ncbi.nlm.nih.gov/pubmed/26303777. Accessed February 13, 2019.

Campbell, M.A., Kan, J.A.L. van, Slot, J.C., Staats, M., and Rokas, A. (2013) Repeated loss of an anciently horizontally transferred gene cluster in Botrytis. *Mycologia* **105**: 1126–1134.

Campbell, M.A., Rokas, A., and Slot, J.C. (2012) Horizontal Transfer and Death of a Fungal Secondary Metabolic Gene Cluster. *Genome Biol Evol* **4**: 289–293 http://gbe.oxfordjournals.org/cgi/doi/10.1093/gbe/evs011.

Caracuel, Z., Roncero, M.I.G., Espeso, E.A., González-Verdejo, C.I., García-Maceira, F.I., and Pietro, A. Di (2003) The pH signalling transcription factor PacC controls virulence in the plant pathogen Fusarium oxysporum. *Mol Microbiol* **48**: 765–779 http://doi.wiley.com/10.1046/j.1365-2958.2003.03465.x. Accessed June 13, 2018.

Clevenger, K.D., Bok, J.W., Ye, R., Miley, G.P., Verdan, M.H., Velk, T., *et al.* (2017) A scalable platform to identify fungal secondary metabolites and their gene clusters. *Nat Chem Biol* **13**: 895–901.

Clutterbuck, A.J. (1972) Absence of Laccase from Yellow-spored Mutants of Aspergillus nidulans. www.microbiologyresearch.org. Accessed February 19, 2019.

Cove, D. (2015) Kinetic studies of the induction of nitrate reductase and cytochrome c reductase in the fungus Aspergillus nidulans . *Biochem J* **104**: 1033–1039 https://www.sciencedirect.com/science/article/pii/S0926659366801200. Accessed February 9, 2019.

Darken, A.A., Jensen, A.L., and Shij, A.P. (1959) Production of Gibberellic Acid by Fermentation. *Appl Microbiol Biotechnol* **7** https://www.ncbi.nlm.nih.gov/pmc/articles/PMC1057525/pdf/applmicro00325-0033.pdf. Accessed July 19, 2018.

Deutschbauer, A.M., Jaramillo, D.F., Proctor, M., Kumm, J., Hillenmeyer, M.E., Davis, R.W., *et al.* (2005) Mechanisms of haploinsufficiency revealed by genome-wide profiling in yeast. *Genetics* **169**: 1915–1925 http://www.ncbi.nlm.nih.gov/pubmed/15716499. Accessed February 15, 2019.

Espeso, E.A., and Arst, H.N. (2000) On the Mechanism by which Alkaline pH Prevents Expression of an Acid-Expressed Gene. *Mol Cell Biol* **20**: 3355–3363 http://mcb.asm.org/content/20/10/3355.long.

Espeso, E.A., Tilburn, J., Sánchez-Pulido, L., Brown, C. V., Valencia, A., Arst, H.N., and Peñalva, M.A. (1997) Specific DNA recognition by the Aspergillus nidulans three zinc finger transcription factor PacC. *J Mol Biol* **274**: 466–480 https://www.sciencedirect.com/science/article/pii/S0022283697914285?via%3Dihub. Accessed November 1, 2018.

Fischer, Steven M; Dai, Y. (2015) Characterization of Differential Metabolites in Bacteria Using a Q-TOF LC/MS Based Metabolomics Batch Data Analysis Workflow. *Agil Technol* 95051 https://www.agilent.com/cs/library/applications/5991-5706EN.pdf. Accessed February 10, 2019.

Frandsen, R.J.N., Nielsen, N.J., Maolanon, N., Sørensen, J.C., Olsson, S., Nielsen, J., and Giese, H. (2006) The biosynthetic pathway for aurofusarin in Fusarium graminearum reveals a close link between the naphthoquinones and naphthopyrones. *Mol Microbiol* **61**: 1069–1080.

Frandsen, R.J.N., Schütt, C., Lund, B.W., Staerk, D., Nielsen, J., Olsson, S., and Giese, H.

(2011) Two novel classes of enzymes are required for the biosynthesis of aurofusarin in Fusarium graminearum. *J Biol Chem* **286**: 10419–10428 http://www.ncbi.nlm.nih.gov/pubmed/21296881. Accessed December 12, 2018.

Friesen, T.L., Stukenbrock, E.H., Liu, Z., Meinhardt, S., Ling, H., Faris, J.D., *et al.* (2006) Emergence of a new disease as a result of interspecific virulence gene transfer. *Nat Genet* **38**: 953–956 http://www.nature.com/articles/ng1839. Accessed February 26, 2019.

Gasch, A.P., Moses, A.M., Chiang, D.Y., Fraser, H.B., Berardini, M., and Eisen, M.B. (2004) Conservation and evolution of cis-regulatory systems in ascomycete fungi. *PLoS Biol* **2**.

Green, M.R., and Sambrook, J. (2016) Precipitation of DNA with ethanol. *Cold Spring Harb Protoc* **2016**: 1116–1120 http://www.cshprotocols.org/lookup/doi/10.1101/pdb.prot093377. Accessed February 11, 2019.

Hansen, B.G., Salomonsen, B., Nielsen, M.T., Nielsen, J.B., Hansen, N.B., Nielsen, K.F., *et al.* (2011) Versatile Enzyme Expression and Characterization System for Aspergillus nidulans, with the Penicillium brevicompactum Polyketide Synthase Gene from the Mycophenolic Acid Gene Cluster as a Test Case. *Appl Environ Microbiol* **77**: 3044–3051 http://aem.asm.org/cgi/doi/10.1128/AEM.01768-10.

Harvey, C.J.B., Tang, M., Schlecht, U., Horeck, J., Fischer, C.R., Lin, H.-C., *et al.* (2018) HEx: A heterologous expression platform for the discovery of fungal natural products. *Sci Adv* **4**: eaar5459 http://advances.sciencemag.org/lookup/doi/10.1126/sciadv.aar5459. Accessed February 5, 2019.

Holm, D.M.K. (2013) Development and Implementation of Novel Genetic Tools for Investigation of Fungal Secondary Metabolism. .

Husnik, F., and McCutcheon, J.P. (2018) Functional horizontal gene transfer from bacteria to eukaryotes. *Nat Rev Microbiol* **16**: 67–79 https://www.nature.com/articles/nrmicro.2017.137.pdf. Accessed March 26, 2018.

Huß, K., Niehaus, E.-M., Smith, K.M., Proctor, R.H., Hippler, M., Kleigrewe, K., *et al.* (2013) Deciphering the Cryptic Genome: Genome-wide Analyses of the Rice Pathogen Fusarium fujikuroi Reveal Complex Regulation of Secondary Metabolism and Novel Metabolites. *PLoS Pathog* **9**: e1003475 http://dx.plos.org/10.1371/journal.ppat.1003475. Accessed January 25, 2019.

Isobe, T., Motohashi, W., Takahashi, N., Nakayama, H., Taoka, M., Kaji, H., *et al.* (2004) Only a Small Subset of the Horizontally Transferred Chromosomal Genes in Escherichia coli Are Translated into Proteins . *Mol Cell Proteomics* **3**: 780–787 http://www.ncbi.nlm.nih.gov/pubmed/15115803. Accessed February 15, 2019.

Jain, R., Rivera, M.C., and Lake, J.A. (1999) Horizontal gene transfer among genomes: The complexity hypothesis. *Proc Natl Acad Sci* .

Jain, R., Rivera, M.C., Moore, J.E., and Lake, J.A. (2002) Horizontal Gene Transfer in Microbial Genome Evolution. *Theor Popul Biol* **61**: 489–495.

Kaminskyj, S.G.W. (2001) Fundamentals of growth, storage, genetics and microscopy of Aspergillus nidulans. *Fungal Genet Rep* **48**: 25–31 https://doi.org/10.4148/1941-4765.1175. Accessed February 9, 2019.

Keeling, P.J. (2009) Functional and ecological impacts of horizontal gene transfer in eukaryotes. *Curr Opin Genet Dev* **19**: 613–619.

Keller, N.P. (2019) Fungal secondary metabolism: regulation, function and drug discovery. *Nat Rev Microbiol* **17**: 167–180.

Khaldi, N., Collemare, J., Lebrun, M.-H., and Wolfe, K.H. (2008) Evidence for horizontal transfer of a secondary metabolite gene cluster between fungi. *Genome Biol* **9**: R18 http://genomebiology.com/2008/9/1/R18. Accessed February 26, 2019.

Khaldi, N., Seifuddin, F.T., Turner, G., Haft, D., Nierman, W.C., Wolfe, K.H., and Fedorova, N.D. (2010) SMURF: Genomic mapping of fungal secondary metabolite clusters. *Fungal Genet Biol* **47**: 736–41 http://www.ncbi.nlm.nih.gov/pubmed/20554054. Accessed February 26, 2019.

Kim, J.E., Jin, J., Kim, H., Kim, J.C., Yun, S.H., and Lee, Y.W. (2006) GIP2, a putative transcription factor that regulates the aurofusarin biosynthetic gene cluster in Gibberella zeae. *Appl Environ Microbiol* **72**: 1645–1652 http://www.broad.mit.edu/annotation/fungi/fusarium/index.html. Accessed February 21, 2019.

King, R., Urban, M., Hammond-Kosack, M.C.U., Hassani-Pak, K., and Hammond-Kosack, K.E. (2015) The completed genome sequence of the pathogenic ascomycete fungus Fusarium graminearum. *BMC Genomics* **16**: 544 http://www.ncbi.nlm.nih.gov/pubmed/26198851. Accessed January 25, 2019.

Kjærbølling, I., Vesth, T.C., Frisvad, J.C., Nybo, J.L., Theobald, S., Kuo, A., *et al.* (2018) Linking secondary metabolites to gene clusters through genome sequencing of six diverse Aspergillus species. *Proc Natl Acad Sci* **115**: E753–E761 www.pnas.org/cgi/doi/10.1073/pnas.1715954115. Accessed February 26, 2019.

Klitgaard, A., Iversen, A., Andersen, M.R., Larsen, T.O., Frisvad, J.C., and Nielsen, K.F. (2014) Aggressive dereplication using UHPLC-DAD-QTOF: Screening extracts for up to 3000 fungal secondary metabolites. *Anal Bioanal Chem* **406**: 1933–1943 http://link.springer.com/10.1007/s00216-013-7582-x. Accessed February 12, 2019.

Kulak, N.A., Pichler, G., Paron, I., Nagaraj, N., and Mann, M. (2014) Minimal, encapsulated proteomic-sample processing applied to copy-number estimation in eukaryotic cells. *Nat Methods* **11**: 319–324 http://www.nature.com/articles/nmeth.2834. Accessed February 12, 2019.

Landraud, P., Chuzeville, S., Billon-Grande, G., Poussereau, N., and Bruel, C. (2013) Adaptation to pH and Role of PacC in the Rice Blast Fungus Magnaporthe oryzae. *PLoS One* **8**: e69236 http://dx.plos.org/10.1371/journal.pone.0069236. Accessed February 13, 2019.

Larsen, T.O., Rank, C., Frisvad, J.C., Månsson, M., and Nielsen, K.F. (2011) Dereplication of Microbial Natural Products by LC-DAD-TOFMS. *J Nat Prod* **74**: 2338–2348 http://pubs.acs.org/doi/abs/10.1021/np200254t. Accessed February 9, 2019.

Lawrence, J. (1999) Selfish operons: The evolutionary impact of gene clustering in prokaryotes and eukaryotes. *Curr Opin Genet Dev* **9**: 642–648.

Lawrence, J.G. (2003) Gene Organization: Selection, Selfishness, and Serendipity. *Annu Rev Microbiol* **57**: 419–440 http://www.annualreviews.org/doi/10.1146/annurev.micro.57.030502.090816.

Lercher, M.J., and Pál, C. (2007) Integration of Horizontally Transferred Genes into Regulatory Interaction Networks Takes Many Million Years. *Mol Biol Evol* **25**: 559–567 https://academic.oup.com/mbe/article-abstract/25/3/559/1060663. Accessed February 15, 2019.

Lind, A.L., Wisecaver, J.H., Smith, T.D., Feng, X., Calvo, A.M., and Rokas, A. (2015) Examining the Evolution of the Regulatory Circuit Controlling Secondary Metabolism and Development in the Fungal Genus Aspergillus. *PLOS Genet* **11**: e1005096 http://www.ncbi.nlm.nih.gov/pubmed/25786130%5Cnhttp://dx.plos.org/10.1371/journal.pgen.1005096.

Linnemannstöns, P., Schulte, J., Mar Prado, M. Del, Proctor, R.H., Avalos, J., and Tudzynski, B. (2002) The polyketide synthase gene pks4 from Gibberella fujikuroi encodes a key enzyme in the biosynthesis of the red pigment bikaverin. *Fungal Genet Biol* **37**: 134–148.

Ma, L.-J., Does, H.C. van der, Borkovich, K. a, Coleman, J.J., Daboussi, M.-J., Pietro, A. Di, *et al.* (2010) Comparative genomics reveals mobile pathogenicity chromosomes in Fusarium. *Nature* **464**: 367–373.

Medentsev, A.G., Arinbasarova, A.Y., and Akimenko, V.K. (2005) Biosynthesis of naphthoquinone pigments by fungi of the genus Fusarium. *Appl Biochem Microbiol* **41**: 503–507 http://link.springer.com/10.1007/s10438-005-0091-8. Accessed January 22, 2019.

Nielsen, J.B., Nielsen, M.L., and Mortensen, U.H. (2008) Transient disruption of non-homologous end-joining facilitates targeted genome manipulations in the filamentous fungus Aspergillus nidulans. *Fungal Genet Biol* **45**: 165–170 www.elsevier.com/locate/yfgbi. Accessed February 11, 2019.

Nielsen, J.C., Grijseels, S., Prigent, S., Ji, B., Dainat, J., Nielsen, K.F., *et al.* (2017) Global analysis of biosynthetic gene clusters reveals vast potential of secondary metabolite production in Penicillium species. *Nat Microbiol* **2**: 17044 http://www.nature.com/articles/nmicrobiol201744. Accessed February 26, 2019.

Nielsen, K.F., and Larsen, T.O. (2015) The importance of mass spectrometric dereplication in fungal secondary metabolite analysis. *Front Microbiol* **6**: 71 http://www.ncbi.nlm.nih.gov/pubmed/25741325. Accessed February 9, 2019.

Nielsen, M.L., Albertsen, L., Lettier, G., Nielsen, J.B., and Mortensen, U.H. (2006) Efficient PCR-based gene targeting with a recyclable marker for Aspergillus nidulans. *Fungal Genet Biol* **43**: 54–64 https://www.sciencedirect.com/science/article/pii/S1087184505001398. Accessed February 9, 2019.

Nour-Eldin, H.H., Hansen, B.G., Nørholm, M.H.H., Jensen, J.K., and Halkier, B.A. (2006) Advancing uracil-excision based cloning towards an ideal technique for cloning PCR fragments. *Nucleic Acids Res* **34**.

Novozhilov, A.S., Karev, G.P., and Koonin, E. V. (2005) Mathematical modeling of evolution of horizontally transferred genes. *Mol Biol Evol* **22**: 1721–1732 https://academic.oup.com/mbe/article-lookup/doi/10.1093/molbev/msi167. Accessed February 18, 2019.

Papp, B., Pál, C., and Hurst, L.D. (2003) Dosage sensitivity and the evolution of gene families in yeast. *Trends Ecol Evol Nat J Evol Biol Nat Proc R Soc Lond B Evol J Anim Ecol Genet Metapopulation Biol Ecol Genet Evol Annu Rev Ecol Syst Zoo Biol N J Evol Biol* **17**: 230–241.

Park, C., and Zhang, J. (2012) High expression hampers horizontal gene transfer. In *Genome Biology and Evolution*. Oxford University Press, pp. 523–532 http://www.ncbi.nlm.nih.gov/pubmed/22436996. Accessed February 15, 2019.

Proctor, R.H., Hove, F. Van, Susca, A., Stea, G., Busman, M., Lee, T. van der, *et al.* (2013) Birth, death and horizontal transfer of the fumonisin biosynthetic gene cluster during the evolutionary diversification of *Fusarium*. *Mol Microbiol* **90**: n/a-n/a http://doi.wiley.com/10.1111/mmi.12362.

Richards, T. a., Leonard, G., Soanes, D.M., and Talbot, N.J. (2011) Gene transfer into the fungi. *Fungal Biol Rev* **25**: 98–110 http://dx.doi.org/10.1016/j.fbr.2011.04.003.

Rokas, A., Wisecaver, J.H., and Lind, A.L. (2018) The birth, evolution and death of metabolic gene clusters in fungi. *Nat Rev Microbiol* **16**: 731–744 http://dx.doi.org/10.1038/s41579-018-0075-3.

Rosewich, U.L., and Kistler, H.C. (2000) Role of Horizontal Gene Transfer in the Evolution of Fungi. *Annu Rev Phytopathol* **38**: 325–363.

Sasakura, Y., Ogura, Y., Treen, N., Yokomori, R., Park, S.-J., Nakai, K., *et al.* (2016) Transcriptional regulation of a horizontally transferred gene from bacterium to chordate. *Proc*

R Soc B Biol Sci **283**: 20161712 https://royalsocietypublishing.org/doi/pdf/10.1098/rspb.2016.1712. Accessed February 15, 2019.

Schumacher, J., Gautier, A., Morgant, G., Studt, L., Ducrot, P.-H., Pêcheur, P. Le, *et al.* (2013) A Functional Bikaverin Biosynthesis Gene Cluster in Rare Strains of Botrytis cinerea Is Positively Controlled by VELVET. *PLoS One* **8**: e53729 http://dx.plos.org/10.1371/journal.pone.0053729. Accessed June 25, 2018.

Sheridan, K.J., Dolan, S.K., and Doyle, S. (2015) Endogenous cross-talk of fungal metabolites. *Front Microbiol* **6**: 732 http://journal.frontiersin.org/article/10.3389/fmicb.2014.00732/abstract. Accessed November 26, 2018.

Sieber, C.M.K., Lee, W., Wong, P., Münsterkötter, M., Mewes, H.-W., Schmeitzl, C., *et al.* (2014) The Fusarium graminearum genome reveals more secondary metabolite gene clusters and hints of horizontal gene transfer. *PLoS One* **9**: e110311 http://dx.plos.org/10.1371/journal.pone.0110311.

Slot, J.C., and Rokas, A. (2011) Horizontal Transfer of a Large and Highly Toxic Secondary Metabolic Gene Cluster between Fungi. *Curr Biol* **21**: 134–139 http://linkinghub.elsevier.com/retrieve/pii/S0960982210016519.

Soanes, D., and Richards, T. a (2014) Horizontal gene transfer in eukaryotic plant pathogens. *Annu Rev Phytopathol* **52**: 583–614 http://www.ncbi.nlm.nih.gov/pubmed/25090479.

Sorek, R., Zhu, Y., Creevey, C.J., Francino, M.P., Bork, P., and Rubin, E.M. (2007) Genome-wide experimental determination of barriers to horizontal gene transfer. *Science (80-)* **318**: 1449–1452 http://www.ncbi.nlm.nih.gov/pubmed/17947550. Accessed June 25, 2018.

Sørensen, J.L., Nielsen, K.F., and Sondergaard, T.E. (2012) Redirection of pigment biosynthesis to isocoumarins in Fusarium. *Fungal Genet Biol* **49**: 613–618 https://www.sciencedirect.com/science/article/pii/S1087184512001065?via%3Dihub. Accessed November 26, 2018.

Spraker, J.E., Sanchez, L.M., Lowe, T.M., Dorrestein, P.C., and Keller, N.P. (2016) Ralstonia solanacearum lipopeptide induces chlamydospore development in fungi and facilitates bacterial entry into fungal tissues. *ISME J* **10**: 2317–2330 http://www.nature.com/doifinder/10.1038/ismej.2016.32. Accessed August 2, 2018.

Spraker, J.E., Wiemann, P., Baccile, J.A., Venkatesh, N., Schumacher, J., Schroeder, F.C., *et al.* (2018) Conserved Responses in a War of Small Molecules between a Plant-Pathogenic Bacterium and Fungi. *MBio* **9**: e00820-18 http://www.ncbi.nlm.nih.gov/pubmed/29789359. Accessed June 13, 2018.

Studt, L., Wiemann, P., Kleigrewe, K., Humpf, H.-U., and Tudzynski, B. (2012) Biosynthesis of Fusarubins Accounts for Pigmentation of Fusarium fujikuroi Perithecia. *Appl Environ Microbiol* **78**: 4468–4480 http://aem.asm.org/. Accessed April 2, 2019.

Suárez, T., and Peñalva, M.A. (1996) Characterization of a Penicillium chrysogenum gene encoding a PacC transcription factor and its binding sites in the divergent pcbAB-pcbC promoter of the penicillin biosynthetic cluster. *Mol Microbiol* **20**: 529–540 http://www.ncbi.nlm.nih.gov/pubmed/8736532. Accessed February 13, 2019.

Valkonen, M., Yoon, J., Maruyama, J., Kitamoto, K., Kimura, S., Kikuma, T., *et al.* (2002) Structure of a Major Oligosaccharide of Taka-Amylase A. *Appl Microbiol Biotechnol* **30**: 37178–82.

Veitia, R.A. (2004) Gene dosage balance in cellular pathways: Implications for dominance and gene duplicability. *Genetics* **168**: 569–574.

Vesth, T.C., Brandl, J., and Andersen, M.R. (2016) FunGeneClusterS: Predicting fungal gene clusters from genome and transcriptome data. *Synth Syst Biotechnol* **1** http://www.sciencedirect.com/science/article/pii/S2405805X1530017X.

Vesth, T.C., Nybo, J.L., Theobald, S., Frisvad, J.C., Larsen, T.O., Nielsen, K.F., *et al.* (2018) Investigation of inter- and intraspecies variation through genome sequencing of Aspergillus section Nigri. *Nat Genet* **50**: 1688–1695 https://doi.org/10.1038/s41588-018-0246-1. Accessed February 26, 2019.

Vries, R.P. de, Riley, R., Wiebenga, A., Aguilar-Osorio, G., Amillis, S., Uchima, C.A., *et al.* (2016) *Comparative genomics reveals high biological diversity and specific adaptations in the industrially and medically important fungal genus* Aspergillus .

Watanabe, A., Fujii, I., Sankawa, U., Mayorga, M.E., Timberlake, W.E., and Ebizuka, Y. (1999) Re-identification of Aspergillus nidulans wA gene to code for a polyketide synthase of naphthopyrone. *Tetrahedron Lett* **40**: 91–94 https://ac.els-cdn.com/S0040403998800270/1-s2.0-S0040403998800270-main.pdf?_tid=3f21443e-65f9-4af6-a968-ea5c19536ee4&acdnat=1550591706_47cd8190ab391f9c1abbc2df2ff17bcd. Accessed February 19, 2019.

Weber, T., Nave, M., Takano, E., Chevrette, M.G., Medema, M.H., Schwalen, C.J., *et al.* (2017) antiSMASH 4.0—improvements in chemistry prediction and gene cluster boundary identification. *Nucleic Acids Res* **45**: W36–W41 https://academic.oup.com/nar/article-lookup/doi/10.1093/nar/gkx319. Accessed January 31, 2019.

Wellner, A., and Gophna, U. (2008) Neutrality of foreign complex subunits in an experimental model of lateral gene transfer. *Mol Biol Evol* **25**: 1835–1840 https://academic.oup.com/mbe/article-lookup/doi/10.1093/molbev/msn131. Accessed February 15, 2019.

Westphal, K.R., Wollenberg, R.D., Herbst, F.A., Sørensen, J.L., Sondergaard, T.E., and Wimmer, R. (2018) Enhancing the production of the fungal pigment aurofusarin in Fusarium graminearum. *Toxins (Basel)* **10**: 1–11.

Wiemann, P., Brown, D.W., Kleigrewe, K., Bok, J.W., Keller, N.P., Humpf, H.U., and Tudzynski, B. (2010) FfVel1 and fflae1, components of a velvet-like complex in fusarium fujikuroi, affect differentiation, secondary metabolism and virulence. *Mol Microbiol* **77**: 972–994 http://doi.wiley.com/10.1111/j.1365-2958.2010.07263.x. Accessed June 13, 2018.

Wiemann, P., Willmann, A., Straeten, M., Kleigrewe, K., Beyer, M., Humpf, H.U., and Tudzynski, B. (2009) Biosynthesis of the red pigment bikaverin in Fusarium fujikuroi: Genes, their function and regulation. *Mol Microbiol* **72**: 931–946.

Wisecaver, J.H., and Rokas, A. (2015) Fungal metabolic gene clusters - caravans traveling across genomes and environments. *Front Microbiol* **6**: 1–11 http://journal.frontiersin.org/Article/10.3389/fmicb.2015.00161/abstract.

Wisecaver, J.H., Slot, J.C., and Rokas, A. (2014) The Evolution of Fungal Metabolic Pathways. *PLoS Genet* **10**: e1004816 http://dx.plos.org/10.1371/journal.pgen.1004816.

Tables

Table 1 – Overview of strains used in this study

Strain	Genotype *
Reference (IBT35516)	Δ*wA::argB*, Δ*yA*, *veA1*, Δ*nkuA, IS5:AfpyrG*
Reference+OE	IS4:*AfpyrG*
An_FgAUR (IBT35517)	IS5:*FgAUR-AfpyrG*
An_FgAURΔaurR1	IS5:*FgAUR*, Δ*aurR1::AfpyrG*
An_FgAUR+OE:*aurR1*	IS5:*FgAUR*, IS4:*aurR-AfpyrG*
An_FgAUR+OE:*gip1*	IS5:*FgAUR*, IS2:*gip1-AfpyrG*
An_FgAUR+OE:*aurF*	IS5:*FgAUR*, IS2:*aurF-AfpyrG*
An_FfBIK (IBT35518)	IS5:*FfBIK-AfpyrG*
An_FfBIKΔbik5	IS5:*FfBIK*, Δ*bik5*::*AfpyrG*
An_FfBIKΔpacC	IS5:*FfBIK,* Δ*pacC*::*AfpyrG*

* All strains were constructed starting from IBT35516, derived from base strain IBT29539 *veA1*, *argB2*, *pyrG89*, Δ*nkuA* (Nielsen *et al.*, 2008).
IS2 refers to the locus of integration between loci AN4072 and AN4073 on ChrII, IS4 between loci AN4252 and AN4251 on ChrII, IS5 between loci AN7553 and AN7554 on ChrIV.

Table 2 – Overview of pathway products formed from the bikaverin and aurofusarin gene clusters. Biosynthesis notes of (†) FfBIK according to (Wiemann *et al.*, 2009; Arndt *et al.*, 2015) and (‡) FgAUR following (Frandsen *et al.*, 2006; Frandsen *et al.*, 2011). Chemical structures of compounds can be found in Supplementary Figure 4.

Cluster		Compound	Molecular formula	Notes
FfBIK†	**1**	Pre-bikaverin	$C_{18}H_{12}O_6$	Produced by Bik1 (PKS16)
	2	Oxo-pre-bikaverin	$C_{18}H_{10}O_7$	Converted from (1) by Bik2
	3	Nor-bikaverin	$C_{19}H_{12}O_8$	Converted from (1) by Bik3, Bik2
	4	Bikaverin	$C_{20}H_{14}O_8$	Ultimate product of FfBIK
	5	YWA1	$C_{14}H_{12}O_6$	Product of PKS12
	6	Nor-rubrofusarin	$C_{14}H_{10}O_5$	Converted from (5) by AurZ
FgAUR‡	**7**	Rubrofusarin	$C_{15}H_{12}O_5$	Converted from (6) by AurJ
	8	9-hydroxyrubrofusarin	$C_{15}H_{12}O_6$	Converted from (7) by AurF or GIP1
	9	Dimeric 9-hydroxyrubrofusarin	$C_{30}H_{24}O_{12}$	Dimerization of (8) by GIP1, then oxidation by AurO
	10	Aurofusarin	$C_{30}H_{18}O_{12}$	Ultimate product of *FgAUR*

Table 3 – Overview of the response of the bikaverin gene cluster to various abiotic and biotic cues when in *F. fujikuroi* (Wiemann *et al.*, 2009; Wiemann *et al.*, 2010; Studt *et al.*, 2012), HGT recipient *B. cinerea* (Schumacher *et al.*, 2013; Spraker *et al.*, 2018) and *A. nidulans* (this study). Induction of chlamydospore-like structures in all three strains was previously demonstrated (Spraker *et al.*, 2016).

		F. fujikuroi	***B. cinerea***	***A. nidulans***
Abiotic	Nitrogen excess	*bik* repression *Independent of AreA*	*bik* induction	Unresponsive
	High pH	*bik* repression *Dependent on PacC*	Not reported	*bik* repression *Dependent on PacC*
	Light	Negative regulation by VeA[2]	Positive regulation by VeA[2]	Not studied
Biotic	Exposure to ralsolamycin from *Ralstonia solanacearum*	*bik* induction Chlamydospores induced	*bik* induction Chlamydospores induced	Unresponsive Chlamydospores induced

Figures

Figure 1 – Workflow for the experimental whole-BGC transfer from donor to recipient genome, as a model for HGT. A – PCR amplification of BGCs from donor genome, in 8-10 kb fragments with 1.5 kb overlapping homologous sequences. **B** - One-step assembly of vector for targeted integration of the cluster into the *A. nidulans* genome, and restriction enzyme based liberation of the two targeting cassettes with the BGC flanking regions. **C** – Co-transformation and *in-vivo* assembly of the gene cluster and integration into the recipient genome. **D** – PCR verification of overlapping regions (marked by arrows) followed by high-coverage Illumina sequencing.

Figure 2 – Production of aurofusarin related metabolites following transfer of the aurofusarin cluster to *A. nidulans*. The *An_FgAUR* and reference strains were cultured on YES for 7 days at 37 °C. A- EIC of rubrofusarin and aurofusarin masses in *An_FgAUR* on YES. EIC+(273.0757, 571.0871). **B-** EIC of compounds (**11**) and (**12**) in *An_FgAUR* on YES. EIC+(517.1130, 531.1281, 531.1289)**. C-** Table showing the high resolution MS based measured masses of compounds (**11**), (**12.1**) and (**12.2**), their likely molecular formula, the theoretical mass of the predicted formula and its difference to the measured mass (ppm).

Figure 3 – Extracted Ion Chromatograms (EIC+) of compounds (7), (10), (11), (12.1), (12.2) in strains containing the aurofusarin cluster and an additional copy of *aurR1*, *aurF* or *gip1* under the strong *gpdA* promoter, compared to the strain *An_FgAUR* containing only the aurofusarin cluster. Reference+OE contains an empty overexpression cassette with the *AfpyrG* selection marker. The asterisk refers to compound (7) being present, but not visible as a peak at this scale. Strains were grown on solid YES medium at 37 °C for 7 days. EIC+(273.0757, 517.1130, 531.1289, 571.0871)

Figure 4 – Comparison of aurofusarin pathway transcription and protein levels on solid YES medium before and after *aurR1* overexpression. A- Relative gene expression as log2(fold change) of *An_FgAUR*+OE:*aurR1* compared to *An_FgAUR*. Genes are presented following their order within the aurofusarin gene cluster. Error bars based on technical triplicates**. B-** Protein abundances detected by HPLC-MS in biological duplicate, where – / ± / + / ++ indicate 'peak not found in either sample' / 'peak found in one of two samples' / 'peak found in both samples' / 'peak found in high abundance in both samples', respectively, as calculated using Proteome Discover 2.2 software (Thermo Fisher Scientific).

Figure 5 – Extracted Ion Chromatograms of pathway products in *An_FgAUR*Δ*aurR1* and *An_FfBIK*Δ*bik5* demonstrate activity of clusters after deletion of the respective cluster specific transcription factors. A- EIC of aurofusarin pathway products in the *An_FgAUR*Δ*aurR1* and *An_FgAUR* strains on solid YES and MM media. Asterisk does not correspond do (**7**) as manually confirmed by MS/MS. EIC+(273.0757, 517.1129, 531.1286). **B-** EIC of bikaverin pathway products in the *An_FfBIK*Δ*bik5* and *An_FfBIK* strains on solid YES medium. EIC+(383.0761).

Figure 6 – Effect of pH on expression of bikaverin cluster genes in *An_FfBIK* and PacC deletion mutant *An_FfBIK*Δ*pacC*. A- Bikaverin gene expression on YES medium buffered at pH 4, versus YES medium buffered at pH 8. **B-** Expression of bikaverin genes in the *An_FfBIK*Δ*pacC* deletion mutant compared to the *An_FfBIK* strain. Relative expression is shown as $\log_2$(fold change) using average Ct values of a minimum of 3 biological replicates, cultivation 48h on YES medium. Error bars indicate standard error of biological replicates. Asterisks indicate statistical significance as measured by two-sample T-Test (*, **, ***, **** indicate p-value < 0.05, 0.01, 0.001, 0.0001 respectively). **Differential expression of bikaverin genes when culturing *An_FfBIK* with culture supernatants of *R. solanacearum* GMI1000, the Δ*rmyA* mutant, or CPG blank medium control. C-** Bikaverin gene expression with addition of GMI1000 supernatant versus addition of Δ*rmyA* supernatant. **D-** Expression of bikaverin genes with addition of Δ*rmyA* supernatant compared to addition of CPG medium control. Relative expression is shown as $\log_2$ fold change, measured in technical triplicates.

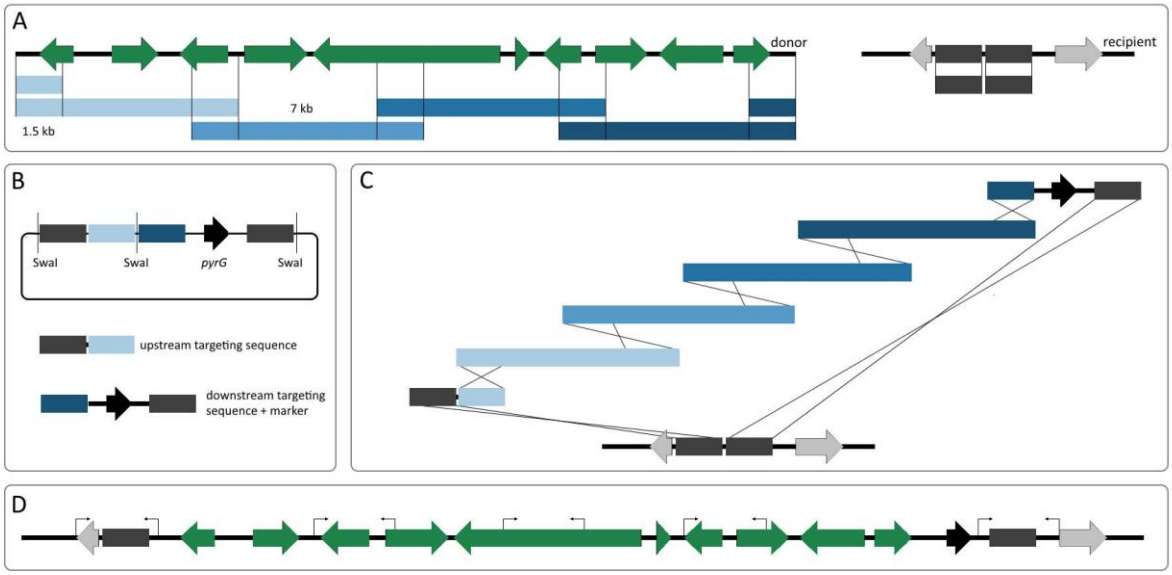

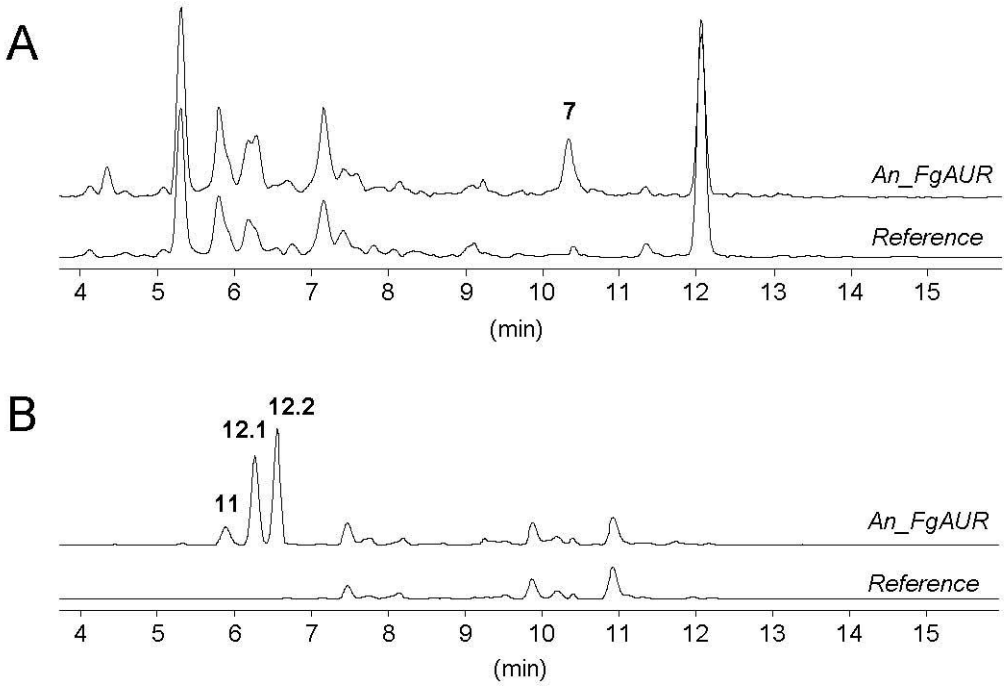

C

	m/z measured		Molecular formula	*m/z theoretical*	Δ (ppm)
11	517.1130	$[M+H]^+$	$C_{28}H_{20}O_{10}$	517.1129	0.19
12.1	531.1289	$[M+H]^+$	$C_{29}H_{22}O_{10}$	531.1286	0.56
12.2	531.1281	$[M+H]^+$	$C_{29}H_{22}O_{10}$	531.1286	0.94

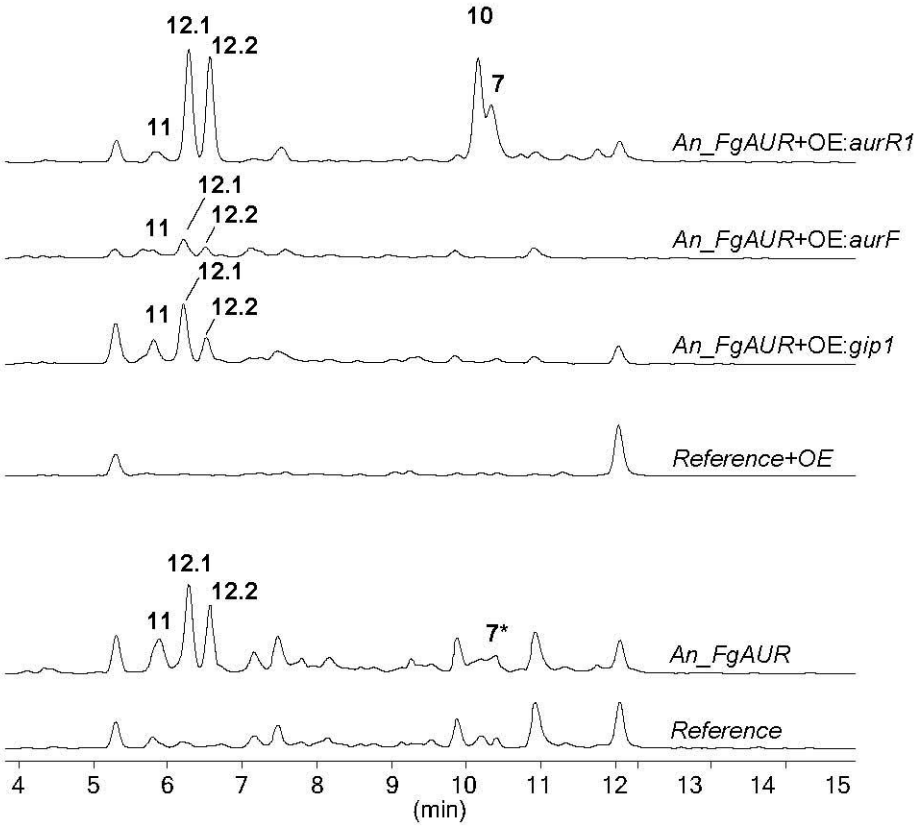

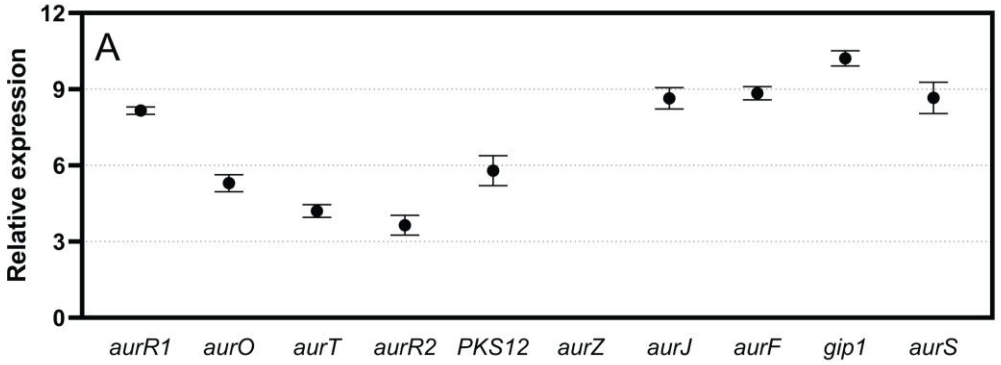

Protein abundance

B

	AurR1	AurO	AurT	AurR2	PKS12	AurZ	AurJ	AurF	Gip1	AurS
An_FgAUR	±	++	-	-	++	+	+	+	+	+
An_FgAUR +OE:aurR1	++	++	+	-	++	++	++	++	++	++

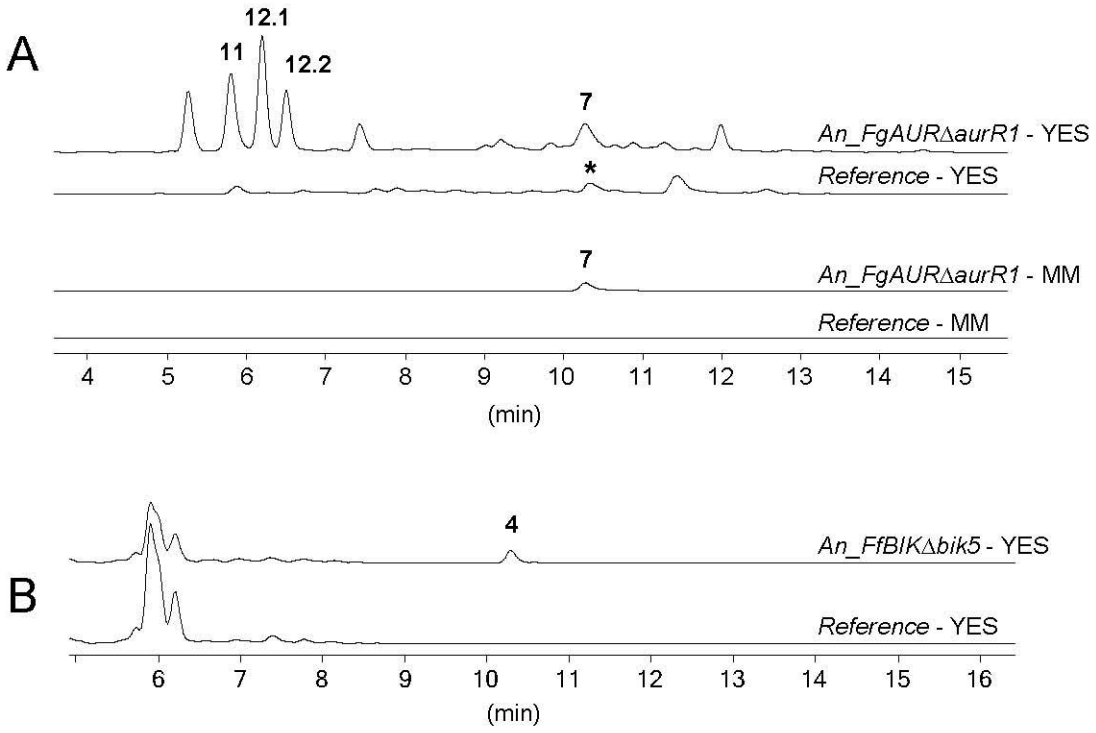

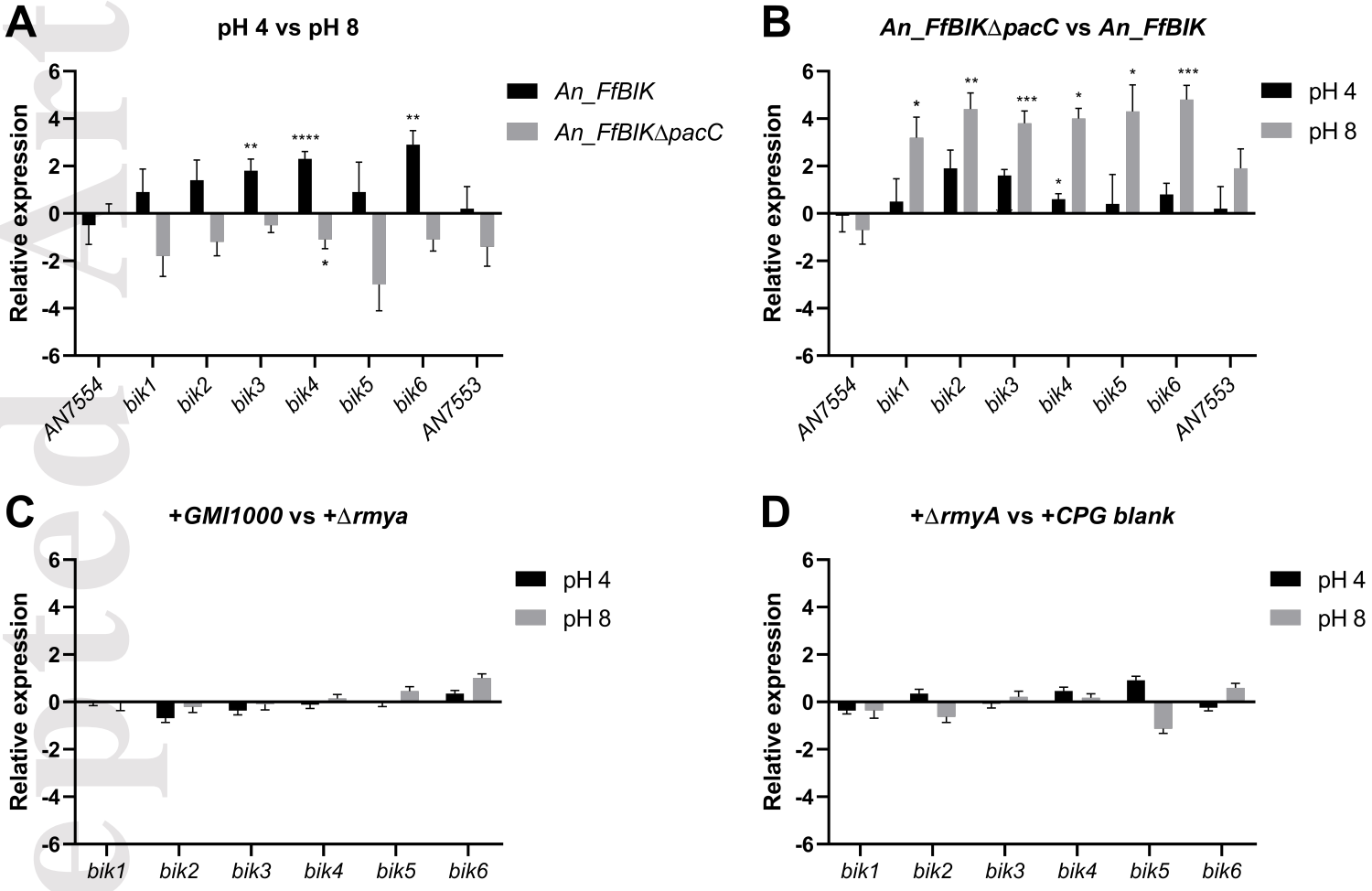
A
pH 4 vs pH 8
Relative expression
An_FfBIK
An_FfBIKΔpacC
AN7554
bik1
bik2
bik3
bik4
bik5
bik6
AN7553
B
An_FfBIKΔpacC vs An_FfBIK
pH 4
pH 8
C
+GMI1000 vs +Δrmya
D
+ΔrmyA vs +CPG blank